Project funded by EUROPEAN UNION

LitOUTer
Raising Public Awareness and Reducing Marine Litter for Protection of the Black Sea Ecosystem Project

Black Sea CROSS BORDER COOPERATION

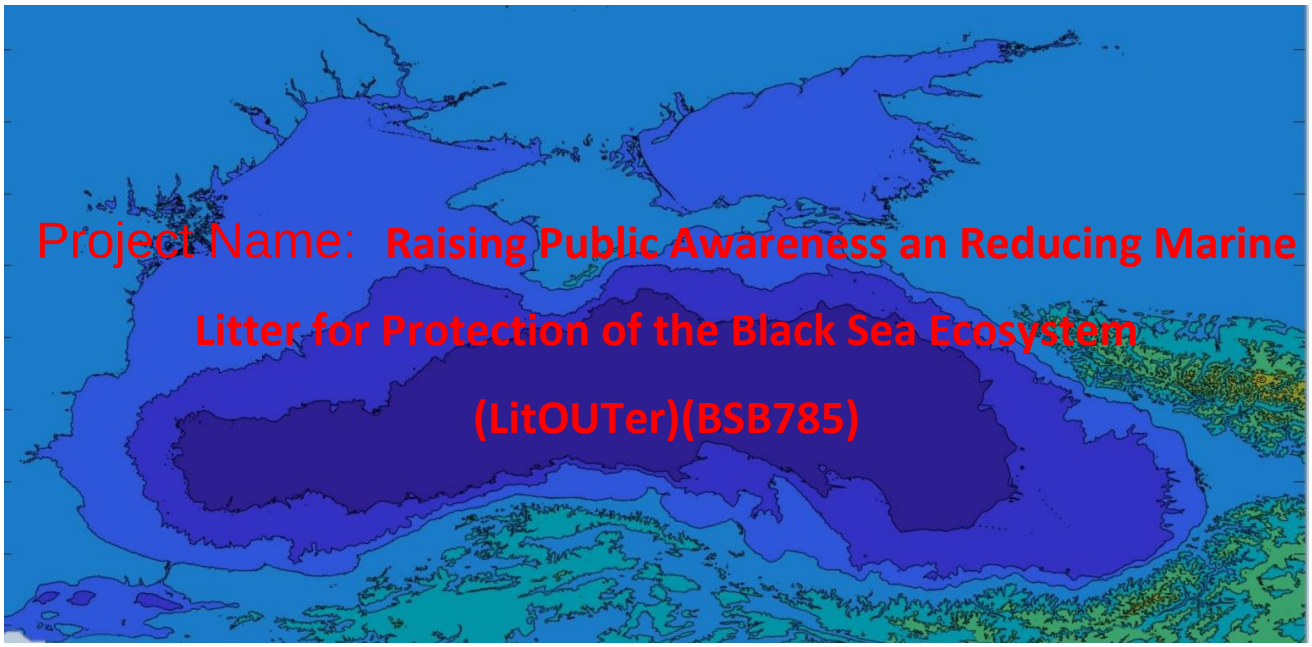

Project Name: Raising Public Awareness an Reducing Marine Litter for Protection of the Black Sea Ecosystem (LitOUTer)(BSB785)

First Report

Contract MLPDA 88652/26.06.2020

Reporting Date
20.09.2022

Project coordinator: Doç.Dr. Coşkun ERÜZ

Project website: https://litouterproject.eu/

Prepared by DATAKENT Bilgisayar Yazılım Eğitim ve Servis Hizmetleri Ltd.Şti.

Trabzon 2022

Table of Contents

List of Figures

List of Tables

1 GENERAL INFORMATION ABOUT PROJECT

The modelling study is a part of the LitOUTer (CBC BSB-785) project (GA.T.3.). The main goal of the project is to raise public awareness with many educational/training materials such as training, play cards, animations, toys, leaflets/brochures and also modelling (litter movement modelling). This report is related to the modelling studies on the litter movements that consisted of some rivers discharging the Black Sea and also coastal areas of the Black Sea.

The sources of the solid wastes along the River basin will be determined. It will be assumed that, the excess amount of the collected solids wastes may reach to the sea via rivers. This will be added to the sources of the litter hot spots in the sea. In addition to that, coastal facilities such as industrial discharges, domestic discharges etc., will be accepted as another hot spots in the sea. Under the light of these information, model will be run to identify relationship between sources and final destination of the litter.
GIS/web based demonstrations will be developed to raise public awareness. Web based model will be based on the general currents of Black Sea, and will show how litter can move when they reach to sea. There will be at least 3 scenarios to cover different wind direction selectable by user.

1.1 Contract Objectives

All oceanographic parameters given below will be measured by CTD-current meter equipment for stated time duration, and raw data will be reported in MS EXCEL. Then, a mathematical model will be developed to investigate the hydrodynamic flow around Rivers chosen and surroundings. The management strategies will reveal to show litter accumulations in and around chosen River.

1.2 Projects Structure

The following steps were used to establish the structure of the projects.

- Firstly, a River from each country were selected for modelling (Türkiye: Sürmene, Georgia: Coruhi,Romania: Danube,Bulgaria: Kamchia)
- Then, Simulations were divided into two groups: General and Coastal simulations
- General current distributions of the Black Sea is used to model general litter spread
    - Each River is given different colours for this simulations
    - Probable reaching points of liters comes from each River were estimated
    - Reachment of litters were simulated
- For coastal simulation the following steps were taken:

- Topography of each River area were digitized.
- Topography, litter amount and wind conditions were inputed in Princeton Ocean Model(POM)
- Wind directions were changed (N,NE,E,SE,S,SW,W,NW)
- Litter amount were reduced by 10%, 30%, 70%

2. GENERAL INFORMATION ABOUT RIVERS

2.1 Sürmene River

Sürmene Stream (Formerly: Kora River) is a River located in Sürmene and Köprübaşı districts of Trabzon province, discharging into the Black Sea (Figure 1). 7 hydroelectric power plants located on the River produce a total of 66 MW of energy [1]. The source of the River is about 2300 meters above sea level and the length of the River is about 40 kilometers. The slope of the River is 58% and, the River originating from the Eastern Black Sea Mountains flows in the north direction. The average annual flow of the stream is 230 hm^3 [1].

Figure 1: Sürmene River

2.2 Coruh River

Çoruh (Turkish: Çoruh, Georgian: ჭოროხი Ch'orokhi,) is a river originating from the Mescit Mountains within the borders of Erzurum province in north-eastern Turkey (Figure 2). It flows through the cities of Bayburt, İspir, Yusufeli and Artvin along the Kelkit-Çoruh Fault, reaching

Georgia, and from here, just south of Batumi, a few kilometers north of the Turkey-Georgia border then, it discharges into the Black Sea. [2]

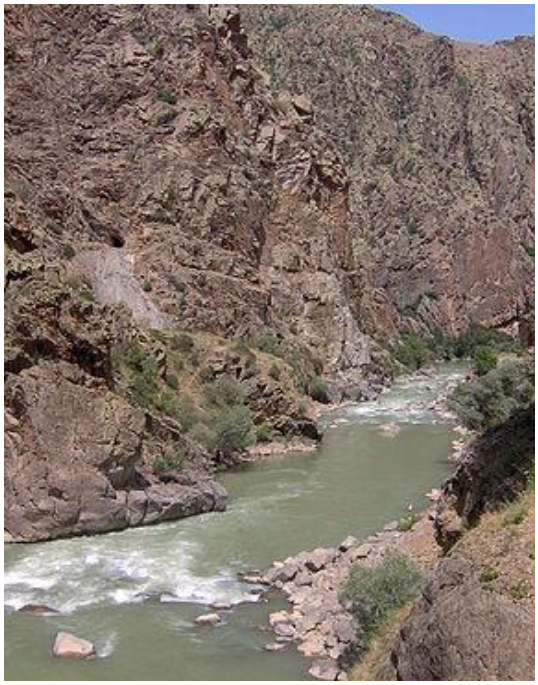

Figure 2: Çoruh River

2.2.1 Çoruh Basin

Çoruh River takes its source from the western face of the Masjid Mountain (3,255 m). First, it flows in the west direction and after passing through Bayburt and İspir. It draws an arc and enters the provincial borders of Artvin in front of the Yokuşlu Village of Yusufeli. After passing through Yusufeli, Artvin and Borcka, it passes through Muratli town of Borcka, leaves the provincial and country borders here and pours into the Black Sea in Batumi (The length from its source to the point where it empties into the sea is 466 km). It empties into the Black Sea in the south of Batumi Port. The part on the territory of Turkey is 442 km, while the remaining part of the territory of Georgia is 24 km. The River has a basin of 19,748 km^3, which corresponds to 2,53% of Turkey's land. In the River basin, there are lands in the provinces of Artvin, Gümüşhane, Erzurum, Bayburt, Kars and Erzincan (Figure 3).

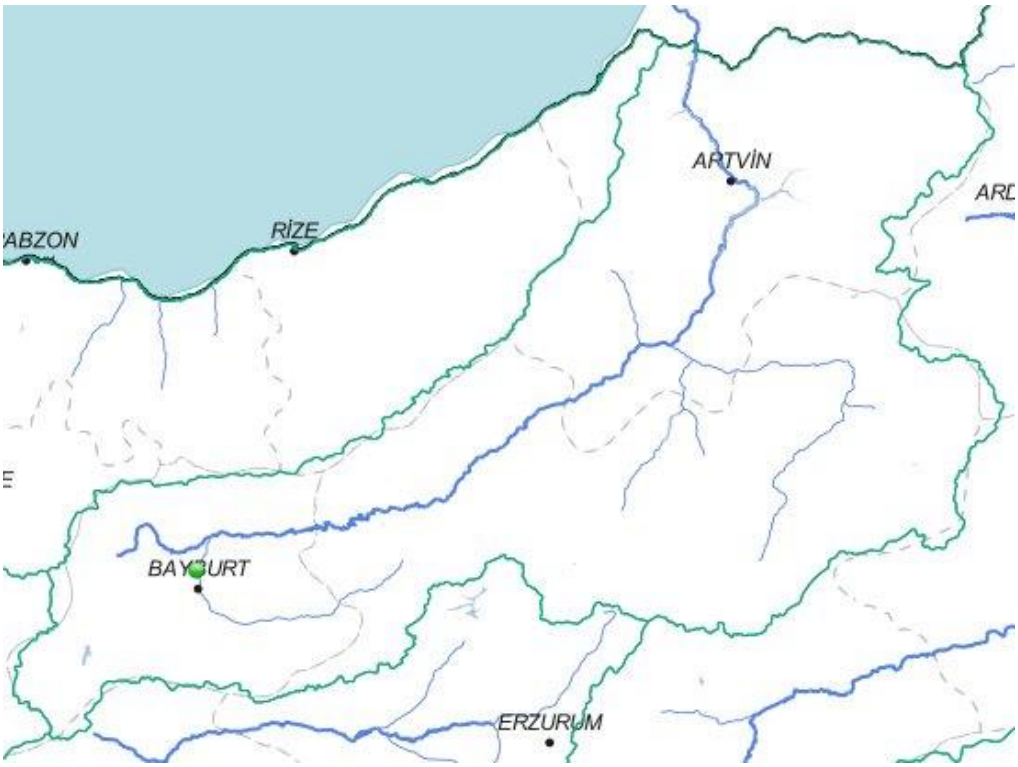

Figure 3: Coruh Basin [2]

2.2.2 Physical Properties of Çoruh River

With a total length of 431 km, 410 km of Coruh is located in Turkey and 21 km in Georgia. The flow rate of Çoruh reaches its peak in May (569/529 m^3/sec,). The lowest flow rate throughout the year is 53,09 m^3/sec. Annual average flow rate is 192 m^3/sec and, the annual average water carrying capacity is 6,3 billion m^3. Çoruh has a high hydroelectric potential with its energy generating head of 1420 meters. The River carries 5,8 million m^3 of sediments per year to the Black Sea. The slope is 5% [3],

2.3 Danube River

Travel along the Danube River to see how it connects the Balkan region to the rest of Europe (Figure 4). The Danube River links the countries of the Balkan Peninsula to each others and to the rest of Europe. Danube River, German Donau, Slovak Dunaj, Hungarian Duna, Serbo-Croatian and Bulgarian Dunav, Romanian Dunărea, Ukrainian Dunay River, the second longest in Europe after the Volga. It rises in the Black Forest mountains of western Germany and flows about 1,770 miles

(2,850 km) to its mouth on the Black Sea. Along its course it passes through 10 countries: Germany, Austria, Slovakia, Hungary, Croatia, Serbia, Bulgaria, Romania, Moldova, and Ukraine [4].

Figure 4: Boats along the Danube River, Belgrade, Serbia,

The Danube played a vital role in the settlement and political evolution of central and southeastern Europe. Its banks, lined with castles and fortresses, formed the boundary between great empires, and its waters served as a vital commercial highway between nations. The River's majesty has been long celebrated in music, The famous waltz *An der schönen, blauen Donau* (1867; *The Blue Danube*), by Johann Strauss the Younger, became the symbol of imperial Vienna. In the 21st century the River has continued its role as an important trade artery. It has been harnessed for hydroelectric power, particularly along the upper courses, and the cities along its banks—including the national capitals of Vienna (Austria), Budapest (Hungary), and Belgrade (Serbia)—have depended upon it for their economic growth.

2.3.1 Physical Properties

The Danube's vast drainage of some 315,000 square miles (817,000 square km) includes a variety of natural conditions that affect the origins and the regimes of its watercourses (Figure 5). They favour the formation of a branching, dense, deep water River network that includes some 300 tributaries, more than 30 of which are navigable. The River basin expands unevenly along its length. It covers about 18,000 square miles (47,000 square km) at the Inn confluence, 81,000 square miles (210,000 square km) after joining with the Drava, and 228,000 square miles (590,000 square km) below the confluences of its most affluent tributaries, the Sava and the Tisza (Figure 6). In the lower course the basin's rate of growth decreases. More than half of the entire Danube

basin is drained by its right-bank tributaries, which collect their waters from the Alps and other mountain areas and contribute up to two-thirds of the total River runoff or outfall.

Figure 5: Danube Basin

Figure 6: The confluence of the Sava (foreground) and Danube Rivers from the Kalemegdan fortress, Belgrade, Serbia,

Three sections are discernible in the River's basin. The upper course stretches from its source to the gorge called the Hungarian Gates, in the Austrian Alps and the Western Carpathian Mountains. The middle course runs from the Hungarian Gates Gorge to the Iron Gate in the Southern Romanian Carpathians. The lower course flows from the Iron Gate to the delta like estuary at the Black Sea.

The upper Danube springs as two small streams—the Breg and Brigach—from the eastern slopes of the Black Forest mountains of Germany, which partially consist of limestone. From Donaueschingen, where the headstreams unite, the Danube flows northeastward in a narrow, rocky bed, to the north rise the wooded slopes of the Swabian and the Franconian mountains. Between Ingolstadt and Regensburg the River forms a scenic canyon-like valley. To the south of the River course stretches the large Bavarian Plateau, covered with thick layers of River deposits from the numerous Alpine tributaries. The bank is low and uniform, composed mainly of fields, peat, and marshland.

At Regensburg the Danube reaches its northernmost point, from which it veers south and crosses wide, fertile, and level country. Shortly before it reaches Passau on the Austrian border, the River narrows and its bottom abounds with reefs and shoals. The Danube then flows through Austrian territory, where it cuts into the slopes of the Bohemian Forest and forms a narrow valley. In order to improve navigation, dams and protecting dikes have been built near Passau, Linz, and Ardagger, The upper Danube, some 600 miles (965 km) long, has a considerable average inclination of the Riverbed (0,93 percent) and a rapid current of two to five miles per hour. Depths vary from 3 to 26 feet (1 to 8 metres). The Danube swells substantially at Passau where the Inn River, its largest upstream tributary, carries more water than the main River. Other major tributaries in the upper Danube course include the Iller, Lech, Isar, Traun, Enns, and Morava Rivers (Figure 7).

Figure 7: Isar River at its source in the Karwendelgebirge (mountains), Bavaria, Germany,

In its middle course the Danube looks more like a flatland River, with low banks and a bed that reaches a width of more than one mile. Only in two sectors—at Visegrád (Hungary) and at the Iron Gate—does the River flow through narrow canyonlike gorges, The basin of the middle Danube exhibits two main features: The flatland of the Little Alfold and Great Alfold plains and the low peaks of the Western Carpathians and Transdanubian Mountains.

The Danube enters the Little Alfold plain immediately after emerging from the Hungarian Gates Gorge near Bratislava, Slovakia. There the River stream slows down abruptly and loses its transporting capacity, so that enormous quantities of gravel and sand settle on the bottom. A principal result of this deposition has been the formation of two islands, one on the Slovak side of the River and the other on the Hungarian side, which combined have an area of about 730 square miles (1,900 square km) that support some 190,000 inhabitants in more than 100 settlements, The silting hampers navigation and occasionally divides the River into two or more channels. East of Komárno the Danube enters the Visegrád Gorge, squeezed between the foothills of the Western Carpathian and the Hungarian Transdanubian Mountains. The steep right bank is crowned with fortresses, castles, and cathedrals of the Hungarian Árpád dynasty of the 10th to 15th century.

Figure 8: Kazan Gorge, cut by the Danube River, on the border of Serbia (left) and Romania,

The Danube then flows past Budapest, and across the vast Great Alfold plain, traversing Croatia, Serbia, and Romania until it reaches the Iron Gate gorge (Figure 8). The Riverbed is shallow and marshy, and low terraces stretch along both banks. River accumulation has built a large number of islands, including Csepel Island near Budapest. In this long stretch the River takes on the waters of its major tributaries—the Drava, the Tisza, and the Sava—which create substantial changes in the River's regime. The average runoff increases from about 83,000 cubic feet (2,400 cubic metres) per second north of Budapest to 200,000 cubic feet (5,600 cubic metres) at the Iron Gate. The River valley looks most imposing there, and the River's depth and current velocity fluctuate widely. The rapids and reefs of the Iron Gate once made the River unnavigable until a lateral navigation channel and a parallel railway allowed Rivercraft to be towed upstream against the strong current.

Beyond the Iron Gate the lower Danube flows across a wide plain; the River becomes shallower and broader, and its current slows down. To the right, above steep banks, stretches the tableland of the Danubian Plain of Bulgaria. To the left lies the low Romanian Plain, which is separated from the main stream by a strip of lakes and swamps. The tributaries in this section are comparatively small and account for only a modest increase in the total runoff. They include the Olt, the Siret, and the Prut (Figure 9). The River is again obstructed by a number of islands. Just south of Cernavodă, the Danube heads northward until it reaches Galați, where it veers abruptly eastward, its left bank briefly traversing Moldovan territory, Near Tulcea, Romania, some 50 miles (80 km) from the sea, the River begins to spread out into its delta.

Figure 9: Olt River, flowing through the Făgăraș Mountains, central Romania

The River splits into three channels: the Chilia, which carries 63 percent of the total runoff, the Sulina, which accounts for 16 percent, and the Sfântu Gheorghe (St, George), which carries the remainder. Navigation is possible only by way of the Sulina Channel, which has been straightened and dredged along its 39-mile (63-km) length. Between the channels, a maze of smaller creeks and lakes are separated by oblong strips of land called *grinduri*. Most *grinduri* are arable and cultivated, and some are overgrown with tall oak forests, A large quantity of reeds that grow in the shallow-water tracts are used in the manufacture of paper and textile fibres, The Danube delta covers an area of some 1,660 square miles (4,300 square km) and is a comparatively young formation. About 6,500 years ago, the delta site was a shallow cove of the Black Sea coast, but it was gradually filled by River-borne silt; the delta continues to grow seaward at the rate of 80 to 100 feet (24 to 30 metres) annually.

2.3.2 Hydrology of Danube River

The different physical features of the River basin affect the amount of water runoff in its three sections. In the upper Danube the runoff corresponds to that of the Alpine tributaries, where the maximum occurs in June when melting of snow and ice in the Alps is the most intensive. Runoff drops to its lowest point during the winter months.

In the middle basin the phases last up to four months, with two runoff peaks in June and April. The June peak stems from that of the upper course, reaching its maximum 10 to 15 days later. The April peak is local and it is caused by the addition of waters from the melting snow in the plains and from the early spring rains of the lowland and the low mountains of the area. Rainfall is important, the period of low water begins in October and reflects the dry spells of summer and autumn that are characteristic of the low plains. In the lower basin, all Alpine traits disappear completely from the River regime. The runoff maximum occurs in April, and the low point extends to September and October.

The River carries considerable quantities of solid particles, nearly all of which consist of quartz grains. The constant shift of deposits in different parts of the Riverbed forms shoals. In the stretches between Bratislava and Komárno and in the Sulina Channel, draglines are constantly at work to maintain the depth needed for navigation. The damming of the River has also changed the way in which sediments are transported and deposited. Water impounded by reservoirs generally loses its silt load, and the water flowing out of the dam—which is relatively silt-free—erodes banks farther downstream.

The temperature of the River water depends on the climate of the various parts of the basin, In the upper course, where the summer waters derive from the Alpine snow and glaciers, the water temperature is low. In the middle and lower reaches, summer temperatures vary between 71 and 75 °F (22 and 24 °C), while winter temperatures near the banks and on the surface drop below freezing. Upstream from Linz the Danube never freezes entirely, because the current is turbulent. The middle and lower courses, however, become icebound during severe winters. Between December and March, periods of ice drift combine with the spring thaw, causing floating ice blocks to accumulate at the River islands, jamming the River's course, and often creating major floods.

The natural regime of River runoff changes constantly as a result of the introduction of stream-regulating equipment, including dams and dikes. The mineral content of the River is greater during the winter than the summer. The content of organic matter is relatively low, but pollution

increases as the waters flow past industrial areas. The River's chemistry also changes as city sewerage and agricultural runoff find their way into the River [4] [5].

2.4 Kamchiya River

The Kamchiya (also Kamchia and Kamčija, Bulgarian: Камчия [ˈkamʧijɐ]) is a 191-kilometre (119 mi) River in eastern Bulgaria,[1] the longest River on the Balkan Peninsula to flow directly into the Black Sea. From its longest source, Golyama Kamchiya (Big Kamchiya), it has a total length of (244.5-kilometre (151.9 mi). The River Kamchiya proper starts from the confluence of the two Rivers springing from Eastern Stara Planina, Golyama Kamchiya (itself formed by the confluence of the Rivers Ticha and Vrana) and Luda Kamchiya (considered major source), flows eastward to the Black Sea and empties into it 25 km south of Varna, in the Resort of Kamchiya.

2.4.1 Physical properties

Running down through Eastern Stara Planina, the Kamchiya meanders through the Longoz or alluvial longose grove, and through the Kamchia (biosphere reserve), a UNESCO-listed biosphere reserve protecting the primeval forest from intensive logging and drainage that had decimated it by mid-20th century. The River mouth forms a sand barrier and often overflows its banks in the valley. The old synclines of the River leave swampy areas called azmatsi. The reserve is 40 km long (stretching throughout the longose grove to the River mouth) and up to 5 km wide (Figure 10).

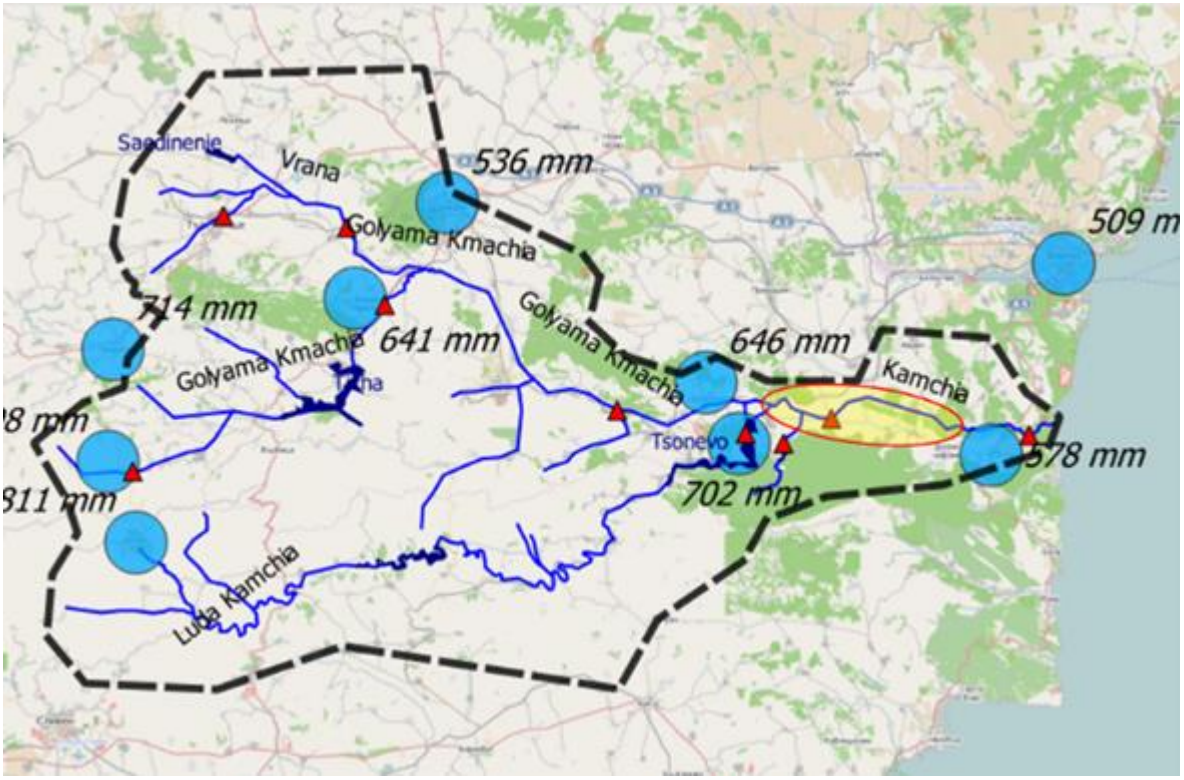

Figure 10: Catchments area of River Kamchiya

The area around the River mouth is remarkable for its (frequently flooded) old growth forests of a Riverine type, up to 450 meter-wide beaches with up to 19 meter-high banks, forested or grass-covered sand dunes, freshwater marshes, and marshy remnants of old Riverbeds, cutting deep into the forest. The unusual coexistence of ash, oak, elm, alder and maple trees, sometimes rising up to 40–50 m with lianas climbing among the branches, creates the impression of a tropical forest, a real tangle of woods. The summer snowflake (Leucojum aestivum) and several buttercup species (Scilla sp.), as well as ferns, grow in the River delta. One can see otter, deer, wild boar and wild cats among the 26 mammal species. There are ospreys, eagles, and up to 200 other bird species, including 56 protected ones, and 25 fish species, among other wildlife. The mouth of the River, as viewed from the south from the Kamchia Biosphere Reserve (Figure 11).

Figure 11: Mouth of River Kamchiya

3 SAMPLING AND MEASURING STRATEGY

3.1 TRABZON-TURKİYE

3.1.1 Sampling

The first sea water masuring (CTD) were done at 5 points of Surmene River off. Coordinates of the sampling stations are given in Table 1 and shown in Figure 12.

Table 1: Coordinates of Sampling Stations

STATION	LONGITUDE (N)	LATITUDE (E)
S1	40˚55'02,71"	40˚06'35,97"
S2	40˚54'58,39"	40˚06' 50,51"
S3	40°55'10.71"	40°06'42.88"
S4	40°55'07.55"	40°06'59.76"
S5	40°55'04.85"	40°07'23.74"

Figure 12: Sampling Stations of Surmene

The first measuring of the following data was done by using Aquadopp IM 300 current to measure currents and Sea Sun Tech, CTD 75 M multi parameter probe was used for oceanographic parameters, Picture of these two equipment are given in Figure 13:.

Figure 13: CTD and current meter used in the sampling provided by the Project coordinator

Raw data is in the attached CD, Continuous data were measured for all oceanographic parameters. Oceanographic parameters were:

- Pressure,
- Temperature,
- Conductivity,
- Salinity,
- Sigma,
- Current Direction and speed

Graphs for temperature, conductivity, salinity, versus depth (sigma) will be given for each stations and others will be given as raw data, Suspended sediment will be given at surface and maximum depth, Current speed and direction at surface, maximum depth and 2 more in between will be shown at each station points on google map given in Figure 12.

3.1.2 Meteorological Data

Precipitation and wind data were obtained from State Meteorological Office, However, wind measurements from land stations underestimate the magnitude of wind above sea surface, This is mainly due to differences in characteristics of the atmospheric planetary boundary layer over land and water, On the basis of theory discussed, wind speed over sea surface was found as

$$U_{sea} = 3.0(U_{land})^{0.67}$$

U_{sea}: Wind speed over sea surface (m/s)

U_{land}: Measured wind speed (m/s)

Table 2: shows the monthly and annual values for the most probable wind speed (Vmp), and the wind speed carrying maximum energy (VmaxE) at height of 10 m, and monthly average wind speed for Trabzon is given in Figure 14:.

Table 2: Meteorological data for Trabzon (DMI)between 1927 - 2020

TRABZON	**Jan**	**Feb**	**March**	**Apr,**	**May**	**June**	**July**	**Aug,**	**Sep,**	**Oct,**	**Nov,**	**Dec,**	**Annual**
	Average values (1927 - 2020)												
Average Temp, (˚C)	7,4	7,3	8,4	11,7	15,9	20,2	23,0	23,4	20,4	16,7	13,0	9,6	14,7
Average Max, Temp, (˚C)	10,8	10,8	12,0	15,5	19,2	23,2	26,0	26,6	23,8	20,1	16,5	13,0	18,1

TRABZON	Jan	Feb	March	Apr,	May	June	July	Aug,	Sep,	Oct,	Nov,	Dec,	Annual
Average Min, Temp, (˚C)	4,7	4,4	5,4	8,7	12,9	17,0	19,9	20,4	17,4	13,7	10,0	6,7	11,8
Average Sun shine (h)	2,7	3,3	3,4	4,4	5,6	7,1	5,9	5,6	4,9	4,5	3,6	2,7	4,5
Average Number of Rainy Day	13,4	12,7	14,1	13,5	14,4	11,7	9,3	10,0	12,0	13,3	12,4	13,0	149,8
Average Total monthly precipitation (kg/m^2)	83,1	64,4	59,2	57,0	52,7	52,0	35,4	48,6	78,5	115,8	98,7	84,6	830,0
	Average Maximum and minimum Temperatures (1927 - 2020)												
Max,Temperature (˚C)	25,9	30,1	35,2	37,6	38,2	36,7	37,0	38,2	37,9	33,8	32,8	26,4	38,2
Min, Temperature (˚C)	-7,0	-7,4	-5,8	-2,0	4,2	9,2	11,0	13,5	7,3	3,4	-1,6	-3,3	-7,4

The diagram for Trabzon shows the days per month, during which the wind reaches a certain speed.

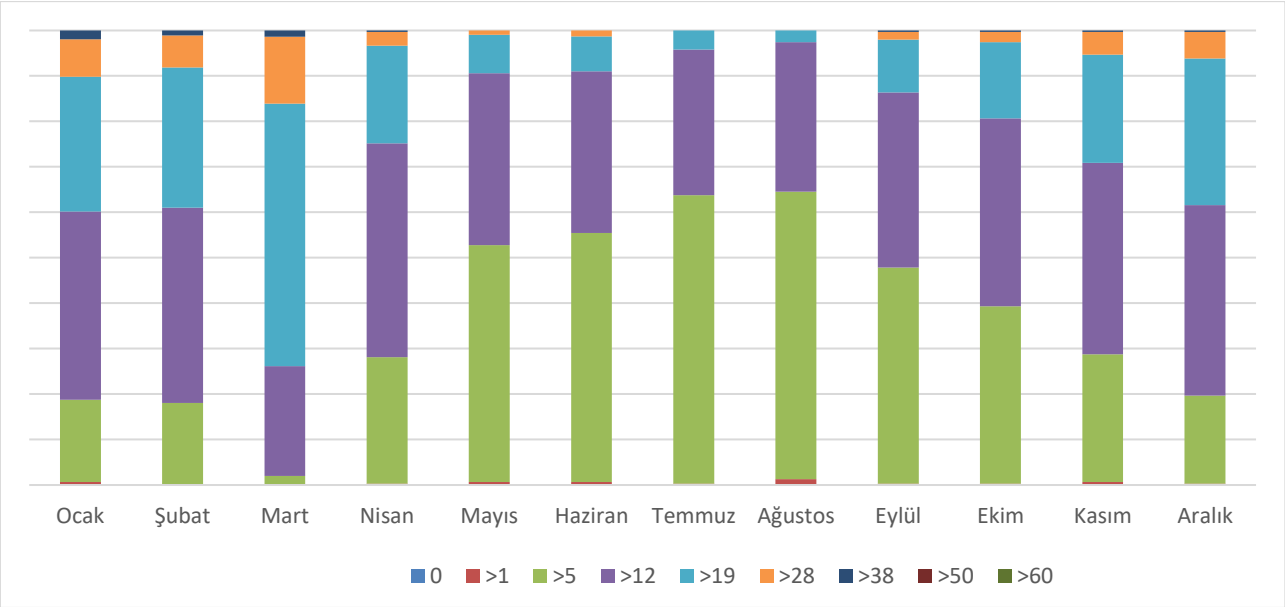

Figure 14: Wind data for Trabzon

The wind rose for Trabzon shows how many hours per year the wind blows from the indicated direction (Figure 15:).

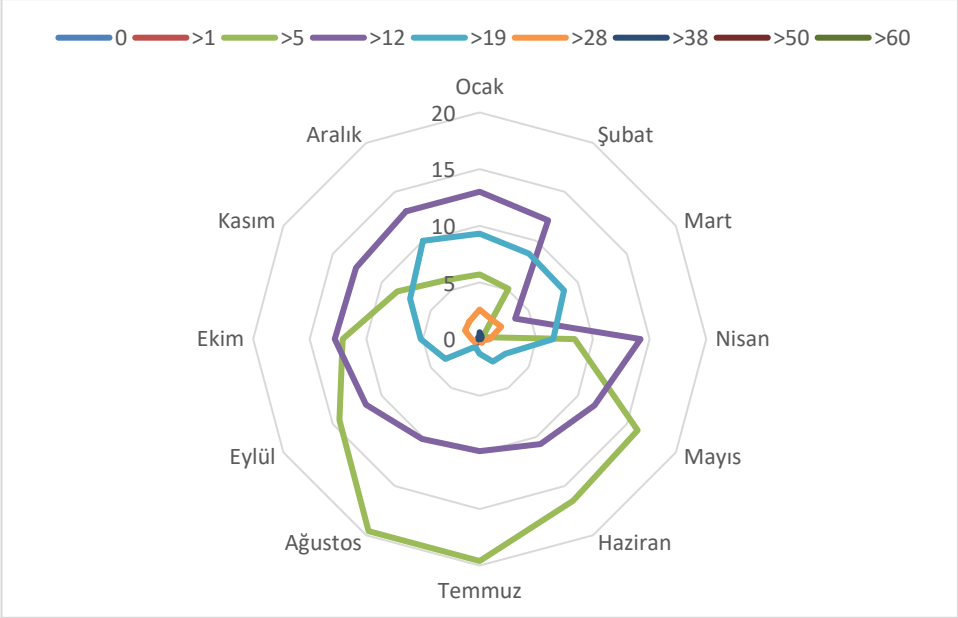

Figure 15: Wind directions and speeds for Trabzon

4 LITTER DISTRIBUTION SIMULATIONS

Four Rivers were selected for simulations. One from each partner countries :

- Surmene River (Turkey)

- Coruhi River (Georgia)
- Danube River (Romania)
- Kamchiya River (Bulgaria)

Fistly, simulations divided in to two: General and Coastal simulations. In general simulations each River and their combinations were simulated. In coastal simulations, each River was simulated in 8 wind direction (N,NE,E,SE,S,SW,W,NW). Then amount of litter was reduced by 10%, 30% and 70% and run simulations with all the conditions mentioned above. Totally 240 simulations were run.

4.1 General current Simulations of Blacksea

For general simulation general Black Sea current as shown in Figure 16:.

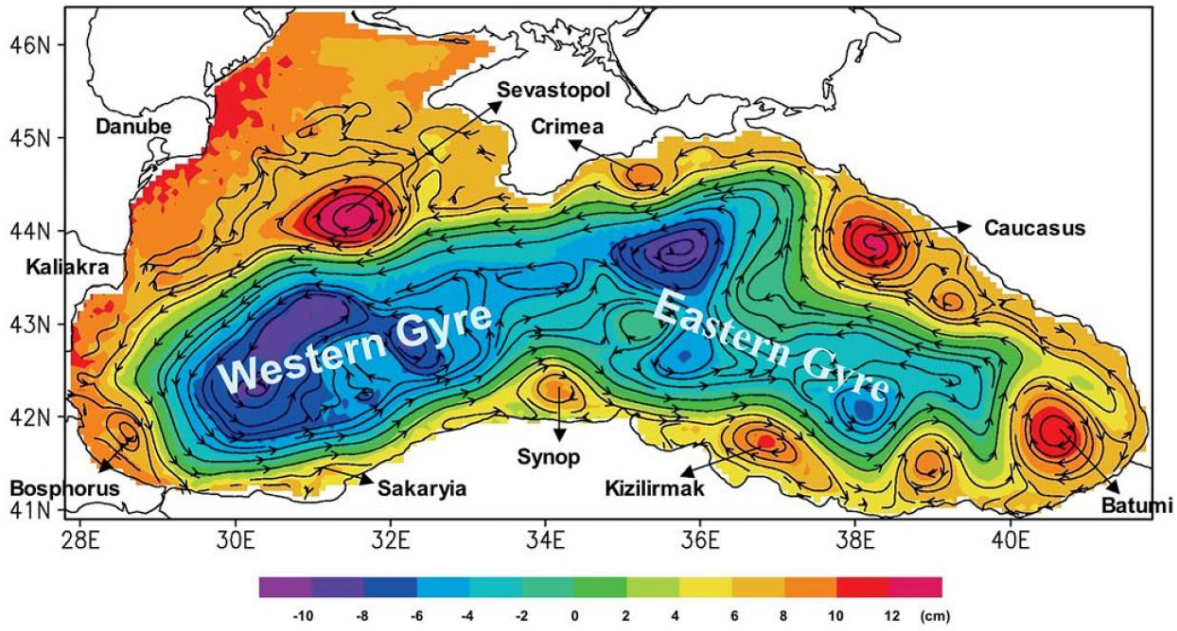

Figure 16: Black Sea surface streamlines (Understanding Black Sea Dynamics by Emil V. Stanev, Oceanography, Vol.18 No.2, 2005)

Four Rivers were simulated as litter input to the Black Sea. Each River simulated with different colours as given in

Table 3:. Combinations of Rivers can be chosen and results can easily be watched. General simulation web page is illustrated in Figure 17:.

Table 3:Simulation colours of each Rivers

Rivers	Colour
Sürmene	Red
Coruhi	Pink
Danube	Orange
Kamchiya	Yellow

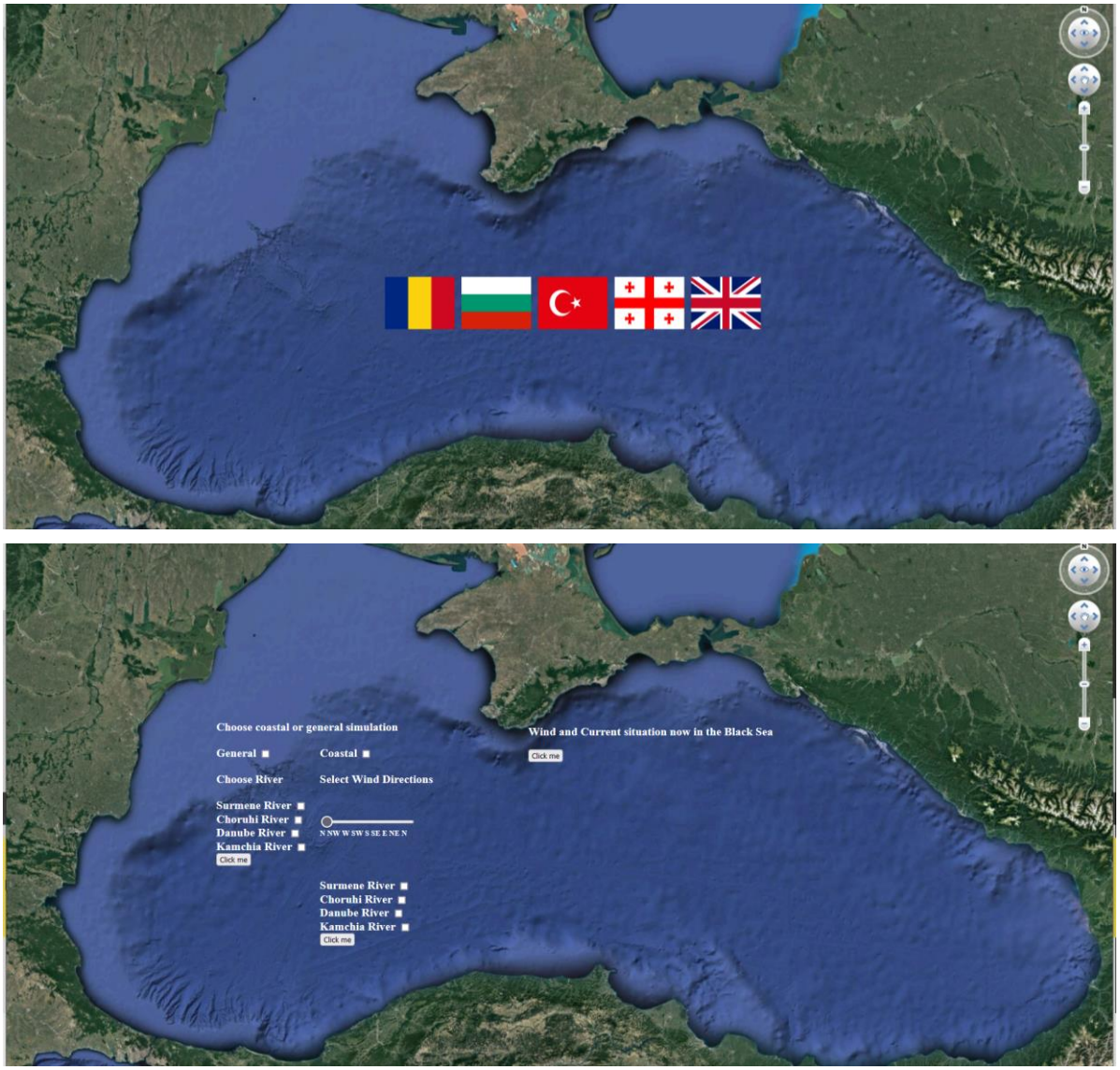

Figure 17: General simulation of litter distribution by Black Sea current system

For example, in general distribution of all rivers (Sürmene, Çoruhi, Danube and Kamchia Rivers) are chosen and “click me” button is clicked (Figure 18 and Figure19). Results are given as follows:

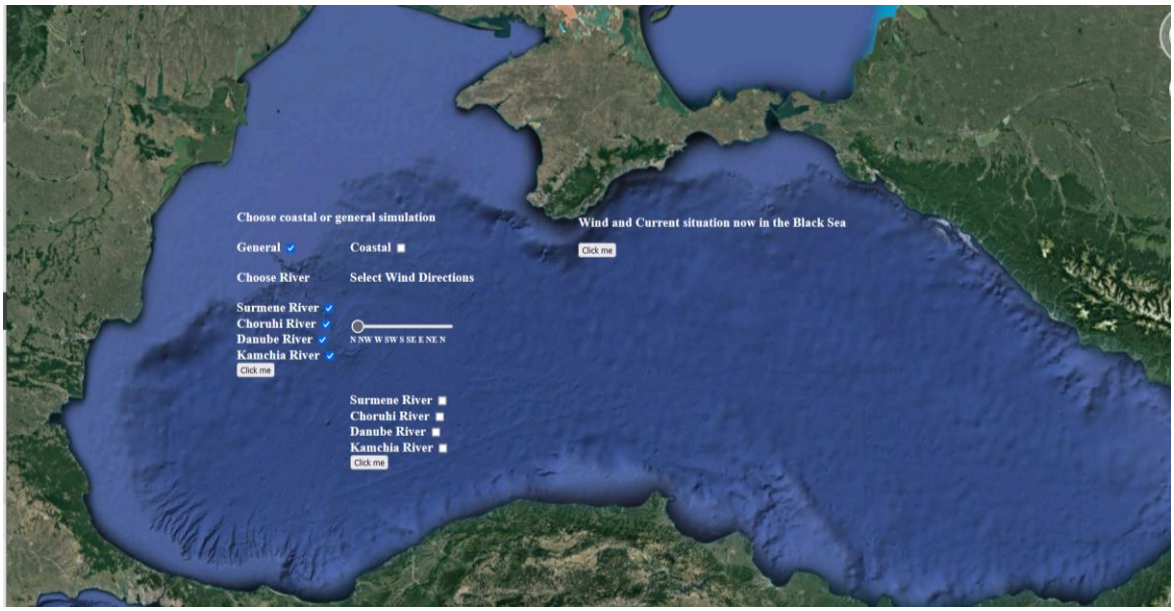

Figure 18: Example for General distribution of 4 Rivers

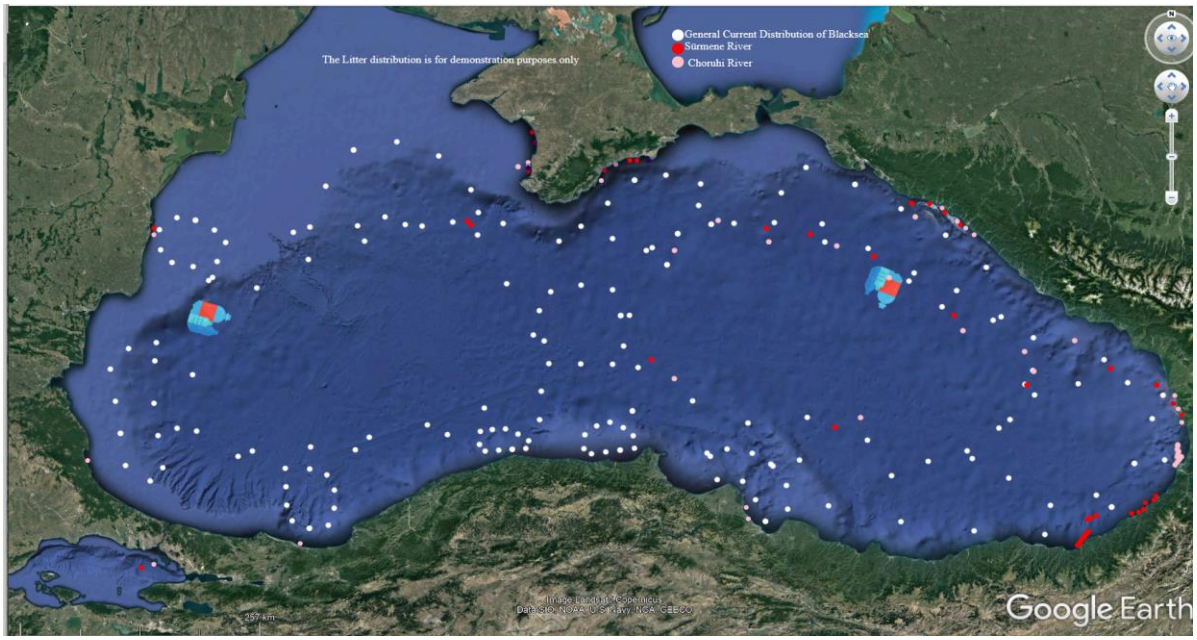

Figure 19: Simulation of Sürmene and Coruhi Rivers in general distribution

If all Rivers are chosen, result is as follows (Figure 20):

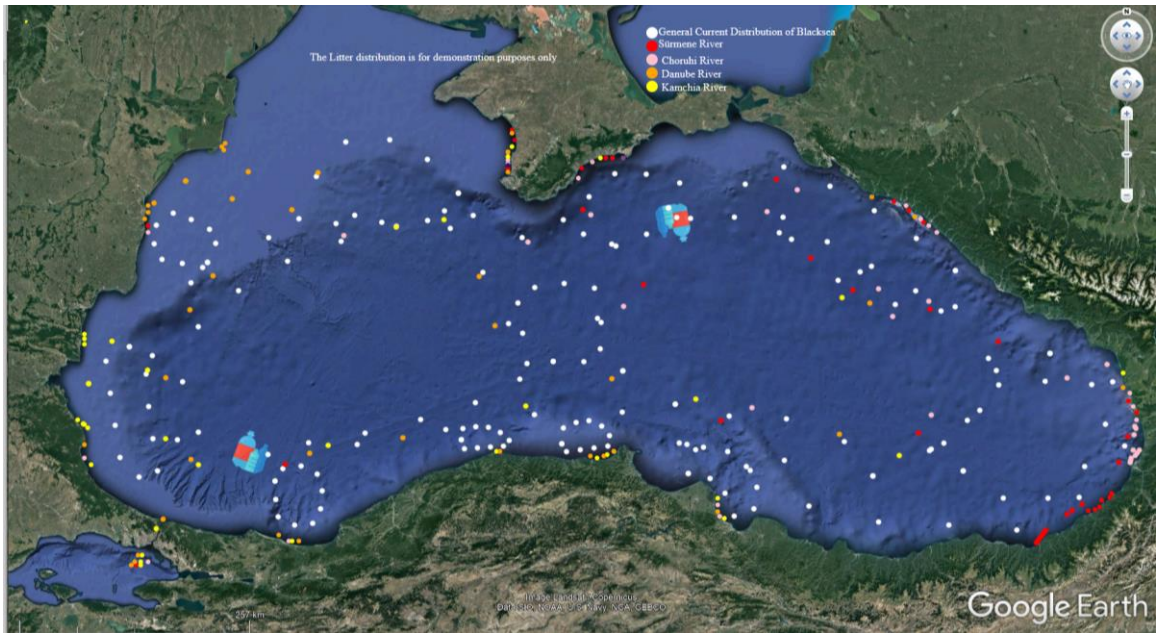

Figure 20: All Rivers in general simulations

4.2 Coastal Simulations

The Coastal simulations was developed based on POMSED model Princeton Ocean Model to simulate current speed, direction and sediment distribution by using, The principal attributes of the model are as follows:

- ✓ It contains an imbedded second moment turbulence closure sub-model to provide vertical mixing coefficients,
- ✓ It is a sigma coordinate model in that the vertical coordinate is scaled on the water column depth,
- ✓ The horizontal grid uses curvilinear orthogonal coordinates and an "Arakawa C" differencing scheme,
- ✓ The horizontal time differencing is explicit whereas the vertical differencing is implicit, The latter eliminates time constraints for the vertical coordinate and permits the use of fine vertical resolution in the surface and bottom boundary layers,
- ✓ The model has a free surface and a split time step, The external mode portion of the model is two dimensional and uses a short time step based on the CFL condition and the external wave speed, The internal mode is three-dimensional and uses a long time step based on the CFL condition and the internal wave speed,
- ✓ Complete thermodynamics have been implemented,

The turbulence closure sub-model is introduced by Mellor, 1973 and then was significantly advanced in collaboration with Tetsuji Yamada (Mellor and Yamada,1974; Mellor and Yamada,1982).

4.2.1 The Basic Equations

Sigma coordinate system has been used for the basic equation. This coordinate system is a bottom following Phillips (1957) or Blumberg and Mellor (1980,1987),

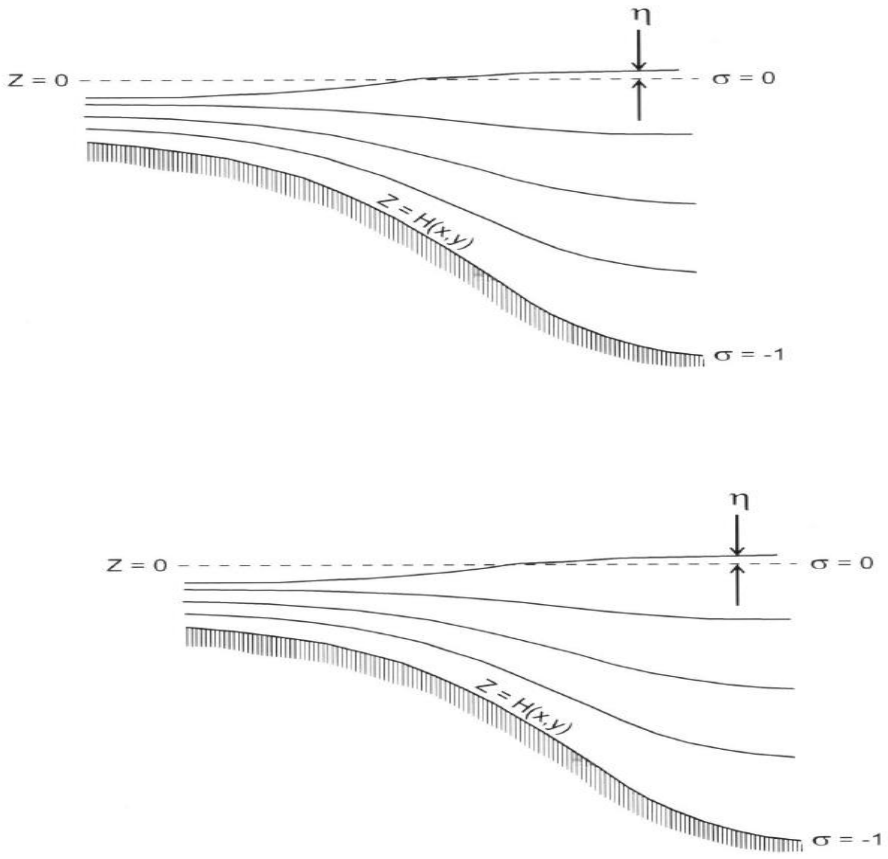

Figure 21: Sigma coordinate system

If internal and external conservative equations is translated from (x,y,z,t) coordinate system to (x*,y*, σ,t*) coordinate system (Figure 21),

$x^* = x$, $y^* = y$, $\sigma = \frac{z-\eta}{H+\eta}$, $t^* = t$, $D \equiv H + \eta$and chain rule implemented,

where

x,y,z are the conventional Cartesian coordinates;

D = H + n where *H* (x, *y*) is the bottom topography

n(x, y, t) is the surface elevation,

Thus, arranges from σ = 0 at z = *n* to σ = -1 at z = -H, After conversion to sigma coordinates and delete of the asterisks, the basic equations may be written (in horizontal Cartesian coordinates),

$$\frac{\partial G}{\partial x} = \frac{\partial G}{\partial x^*} - \frac{\partial G}{\partial \sigma}\left(\frac{\sigma}{D}\frac{\partial D}{\partial x^*} + \frac{1}{D}\frac{\partial \eta}{\partial x^*}\right)$$

$$\frac{\partial G}{\partial y} = \frac{\partial G}{\partial y^*} - \frac{\partial G}{\partial \sigma}\left(\frac{\sigma}{D}\frac{\partial D}{\partial y^*} + \frac{1}{D}\frac{\partial \eta}{\partial y^*}\right)$$

$$\frac{\partial G}{\partial z} = \frac{1}{D}\frac{\partial G}{\partial \sigma}$$

$$\frac{\partial G}{\partial t} = \frac{\partial G}{\partial t^*} - \frac{\partial G}{\partial \sigma}\left(\frac{\sigma}{D}\frac{\partial D}{\partial t^*} + \frac{1}{D}\frac{\partial \eta}{\partial t^*}\right)$$

where$G$ is an arbitrary area and $z = \eta$ for $\sigma = 0$and $z = -H$ for $\sigma = -1$

vertical speed: $\omega \equiv \mathrm{w} - \mathrm{U}\omega\sigma\frac{\partial \mathrm{D}}{\partial \mathrm{x}^*} + \frac{\partial \eta}{\partial \mathrm{x}^*} - \mathrm{V}\sigma\frac{\partial \mathrm{D}}{\partial \mathrm{y}^*} + \frac{\partial \eta}{\partial \mathrm{y}^*} - (\sigma\frac{\partial \mathrm{D}}{\partial \mathrm{t}^*} + \frac{\partial \eta}{\partial \mathrm{t}^*})$

,Boundary conditions :

$$\omega(x^*, y^*, 0, t^*) = 0 \ , \qquad \omega(x^*, y^*, -1, t^*) = 0$$

4.2.2 3-D Advection-Dispersion Equation for Sediment Transportation

$$\frac{\partial C_k}{\partial t} + \frac{\partial U C_K}{\partial x} + \frac{\partial V C_K}{\partial y} + \frac{\partial (W - W_{S,K}) C_K}{\partial z} = \frac{\partial}{\partial x}\left(A_H \frac{\partial C_k}{\partial x}\right) + \frac{\partial}{\partial y}\left(A_H \frac{\partial C_k}{\partial y}\right) + \frac{\partial}{\partial z}\left(K_H \frac{\partial C_k}{\partial z}\right)$$

Where,

U, V, W : 3-D velocity vectors

C_K : Sediment consantration

$W_{S,K}$: Settlement speed

A_H : Horizontal diffusion

K_H : Vertical vorteks diffusion

Boundary conditions :

$$K_H \frac{\partial C_k}{\partial z} = 0 \ , z \to \eta$$

$$K_H \frac{\partial C_k}{\partial z} = E_k - D_K \ , z \to -H$$

E_k: Suspended sediment flux (resuspension)

D_K:Settling flux rate

η : Depth (distance from sea surface)

H :Distance from sea bed

4.2.3 Settlement of Cohesive Sediments

Settlement rate of cohesive sediments depends on the settlement flux rate and their size, According to KRONE, settlement of sediments are as follows:

$$D_{1=-W_{s,1}C_1P_1}$$

$$P_1 = 1 - \frac{1}{\sqrt{2\pi}}\int_{-\infty}^{Y} e^{-\frac{\omega^2}{2}}d\omega$$

$$Y = 2{,}04\log\left[0{,}25\left(\frac{\tau_b}{\tau_{b,min}} - 1\right)e^{1{,}07\tau_{b,min}}\right]$$

where,

D_1 : Settlement flux rate

$W_{s,1}$:Settlement speed of the cohesive sediment

C_1 : Concentration of cohesive suspended sediment

P_1 :Probability of settlement

4.2.4 Re-suspension of Cohesive Sediment

Amount of sediment re-suspends are given with the following formula

$$\varepsilon = \frac{a_0}{T_d^m}\left(\frac{\tau_b - \tau_c}{\tau_c}\right)^n$$

where,

ε:re-suspension potential

a_0:constant depends on source

T_d: time after deposition

τ_b:shear stress of the bed

τ_c:critical shear stress

m, n : constants depends on environment

4.2.5 Calculation of Critical Speed

D_*:Non dimensional parameter for motion

$$\mathrm{D}_* = \left[\frac{(\mathrm{s}-1)\mathrm{g}}{\nu^2}\right]^{\frac{1}{3}}\mathrm{D}_{\mathbf{50}}$$

where,

s: specific gravity

g: acceleration of gravity

ν: Kinematic viscosity

D_{50}: diameter of sediment

According to Shields criteria, critical sliding speed for resuspension is calculated as follows (Figure 22):

$$U_{*,crbed} = [(s-1)gD_{50}\theta_{cr}]^{\frac{1}{2}}$$

θ_{cr}can be calculated as follows;

$$\theta = 0{,}24\ D_*^{-1} D_* \leq 4$$

$$\theta_{cr} = 0{,}14 D_*^{-0{,}64} 40 < D_* \leq 10$$

$$\theta_{cr} = 0{,}04 D_*^{-0{,}10} 10 < D_* \leq 20$$

$$\theta_{cr} = 0{,}13 D_*^{-0{,}29} 20 < D_* \leq 150$$

$$\theta_{cr} = 0{,}055 D_* > 150$$

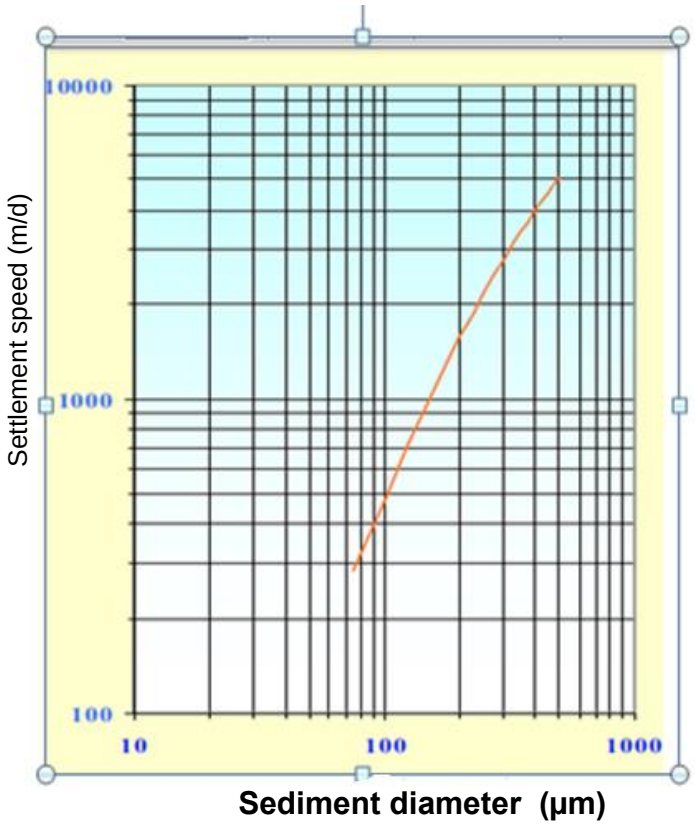

Figure 22: Sediment diameter and settlement speed

4.2.6 Re-suspension of Non- Cohesive Sediment

$$\mathrm{E} = \frac{(\mathrm{sq_s} - \mathrm{qzC_z})\Delta \mathrm{t}}{\Delta \mathrm{x}\Delta \mathrm{y}}$$

where,

C_z: Sediment concentration at minimum sigma level

Δt: time step

$\Delta x \Delta y$:Surface area

$$D_2 = W_{s,2} C_2$$

where,

D_2:Settlement flux rate of non-cohesive sediments

$W_{s,2}$:Settlement speed

C_2:suspended sediment concentrationnear-bed

Simulations were done by using 8 different wind directions (N,NW,W,SW,S,SE,E,NE,N)for each Rivers. All simulations were run for a day. Then, amount of litter were reduced by 10%, 30% and 70%, in order to see their effects.

4.3 Simulations of Sürmene River

In order to simulate coastal currents, topography of the area has to be input in the POM. Therefore, topography of the Sürmene coast was taken from Ref. 1 (https://webapp.navionics.com/?lang=en#boating@6&key=sndyFoyrqF)

4.3.1 Topography of Sürmene River

3-D and contour graphics of topography of Sürmene River is given Figure 23 and Figure 24.

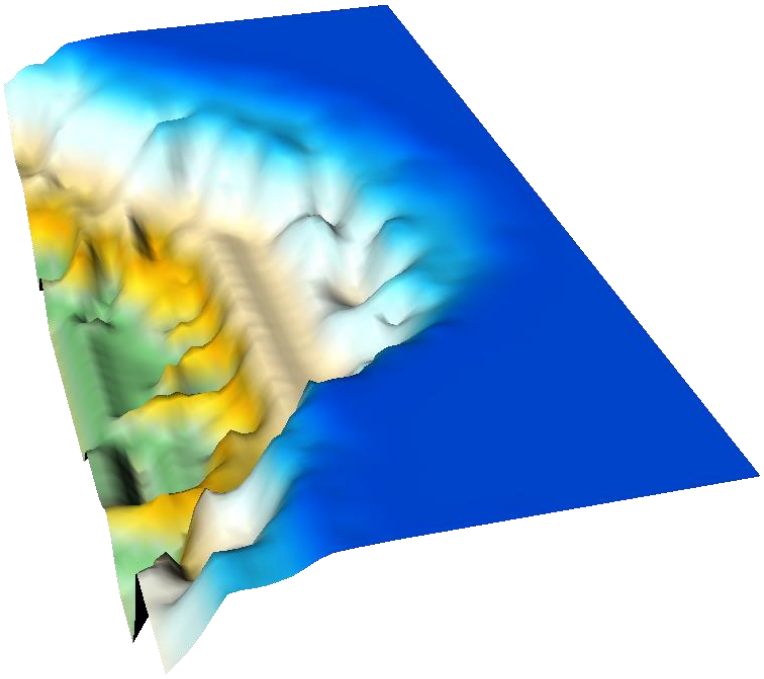

Figure 23: 3-D and contour graphics of topography of Sürmene

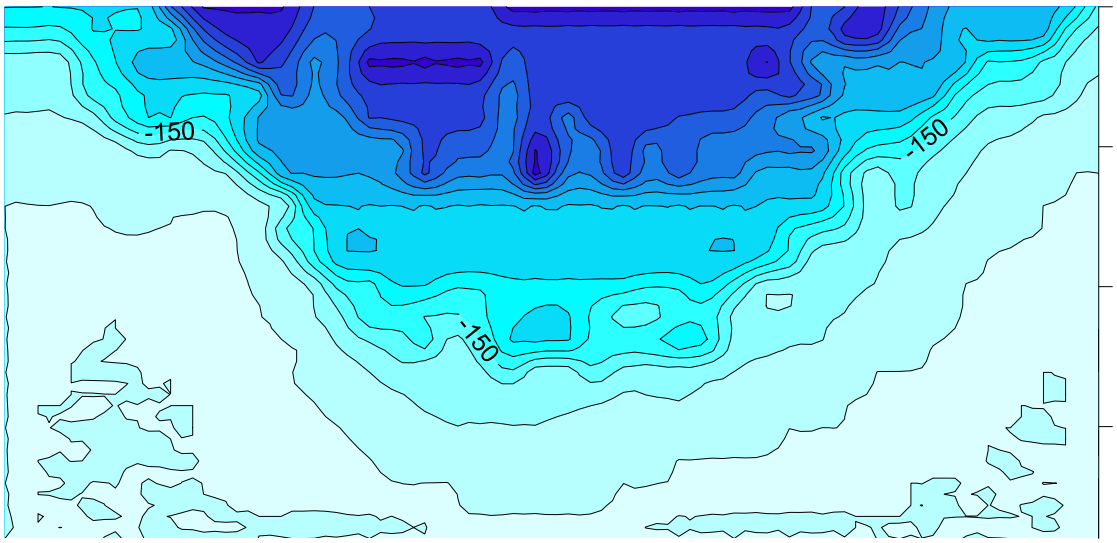

Figure 24: 3D and contour Topography of Sürmene River front

4.3.2 Physical Properties of Seawater in Sürmene River area

Measurements were done on the Sürmene coast at 5 stations. CTD graphs versus depth for each stations are given in the below. Conductivity, Salinity and Temperature results for December is given in Figure 25-29.

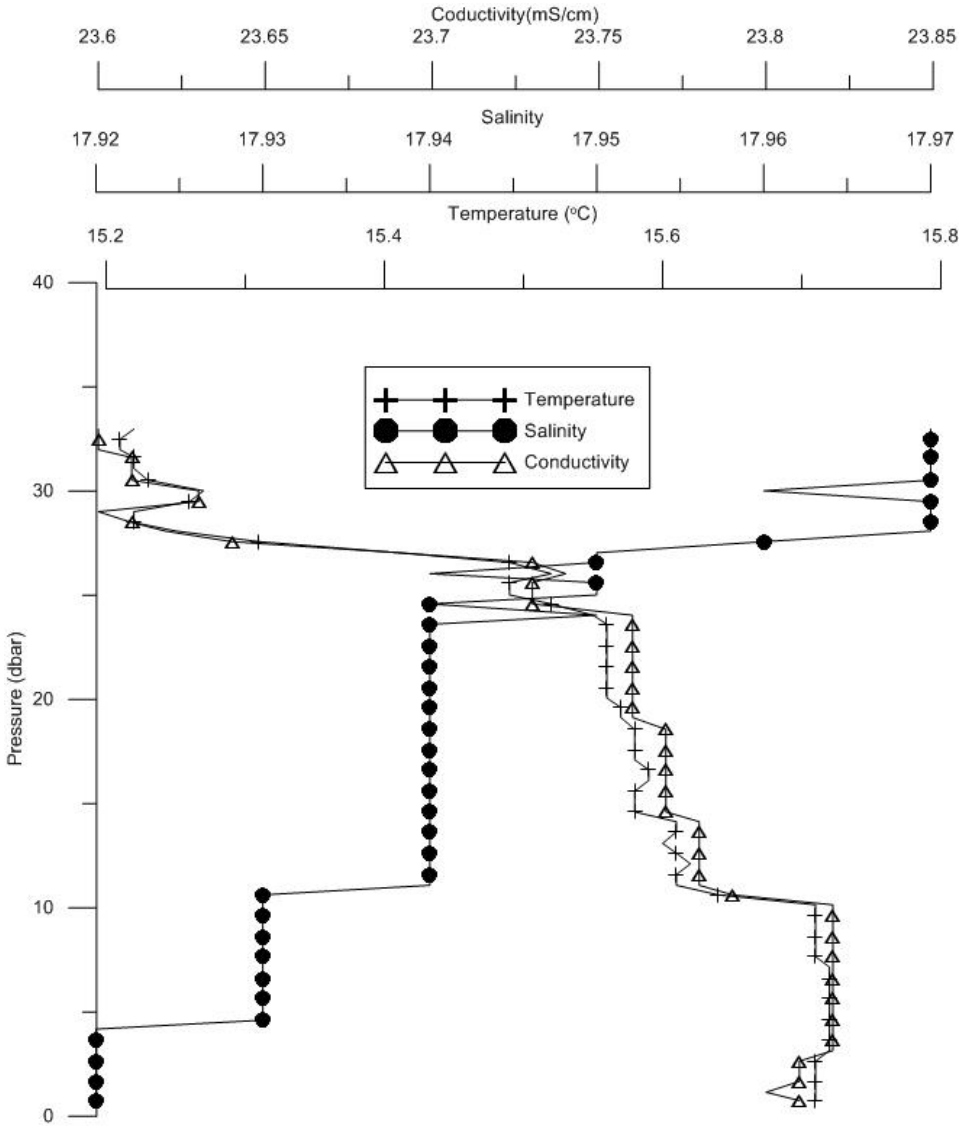

Figure 25: Sampling results of D1 station

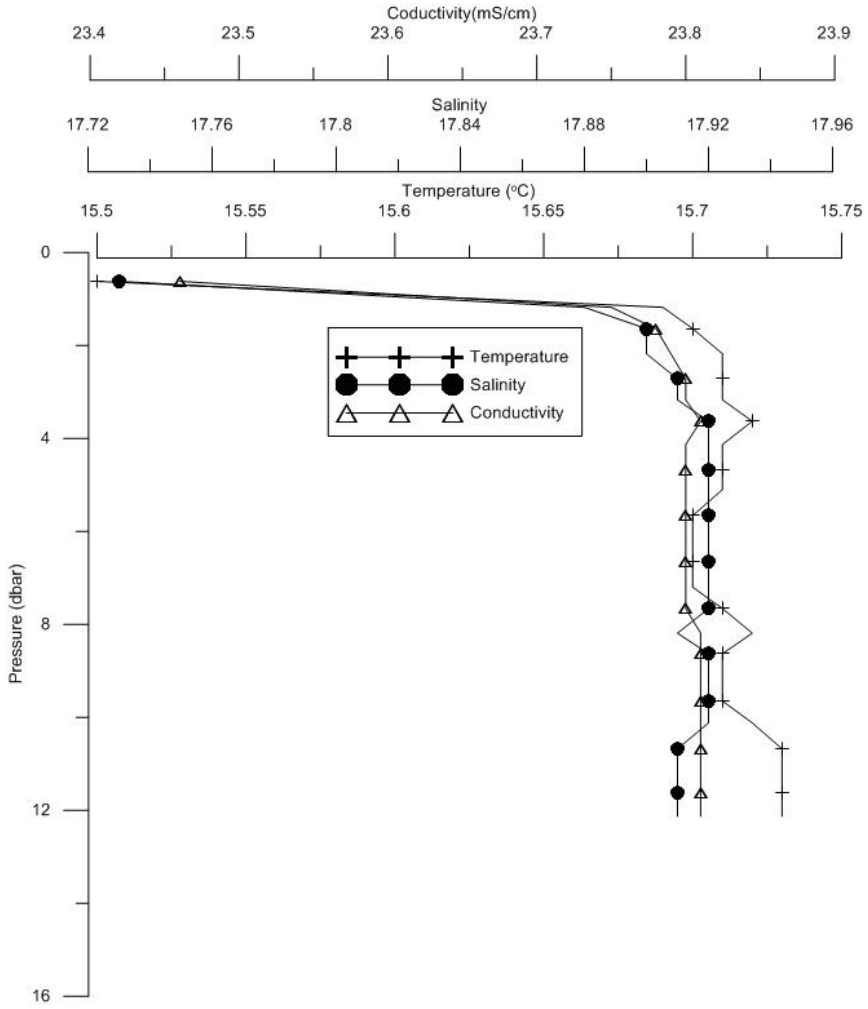

Figure 26: Sampling results of D2 station

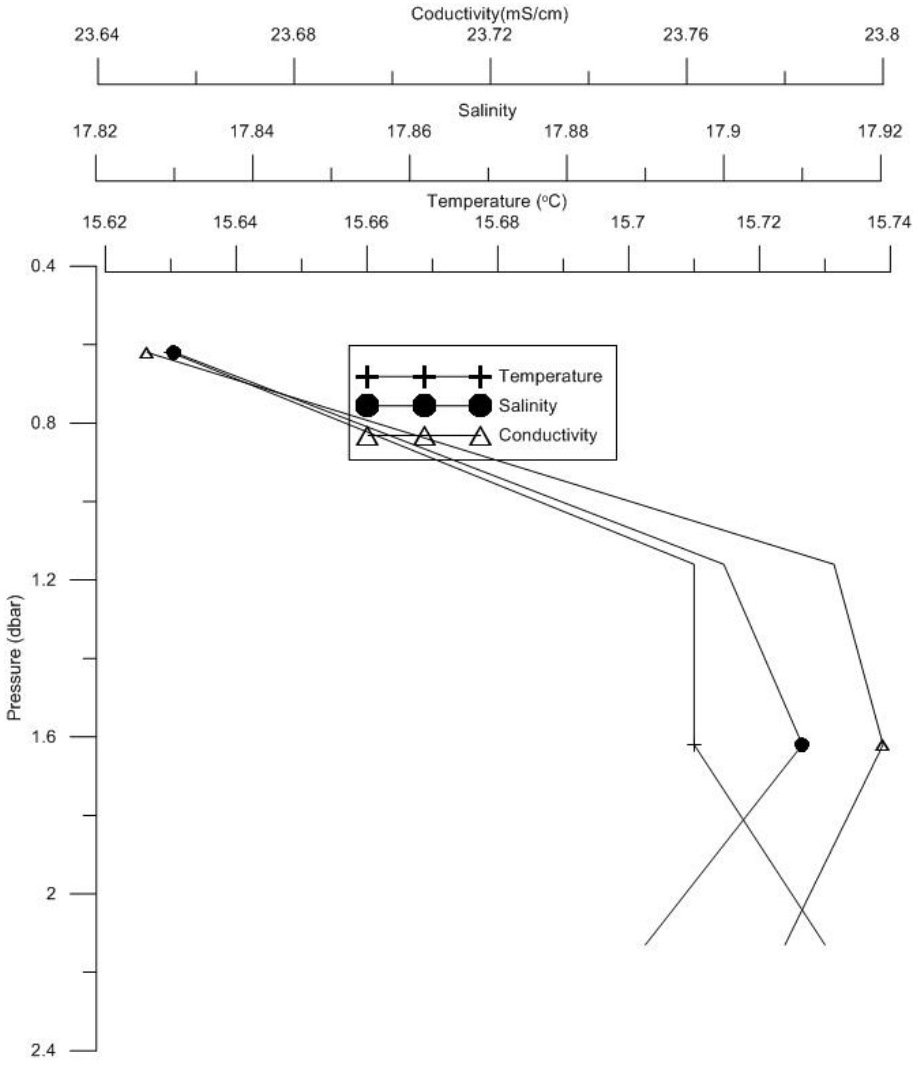

Figure 27: Sampling results of D3 station

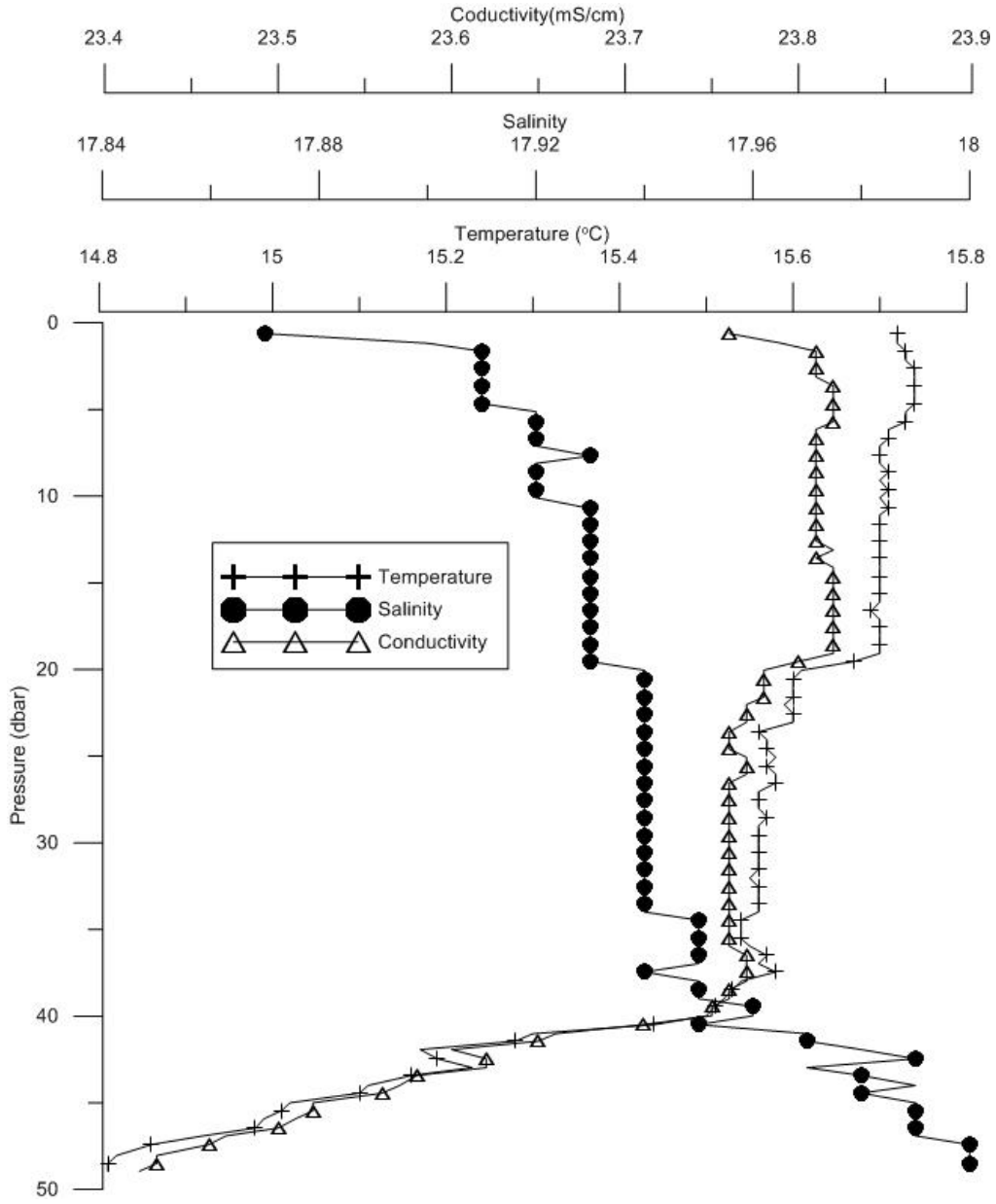

Figure 28: Sampling results of D4 station

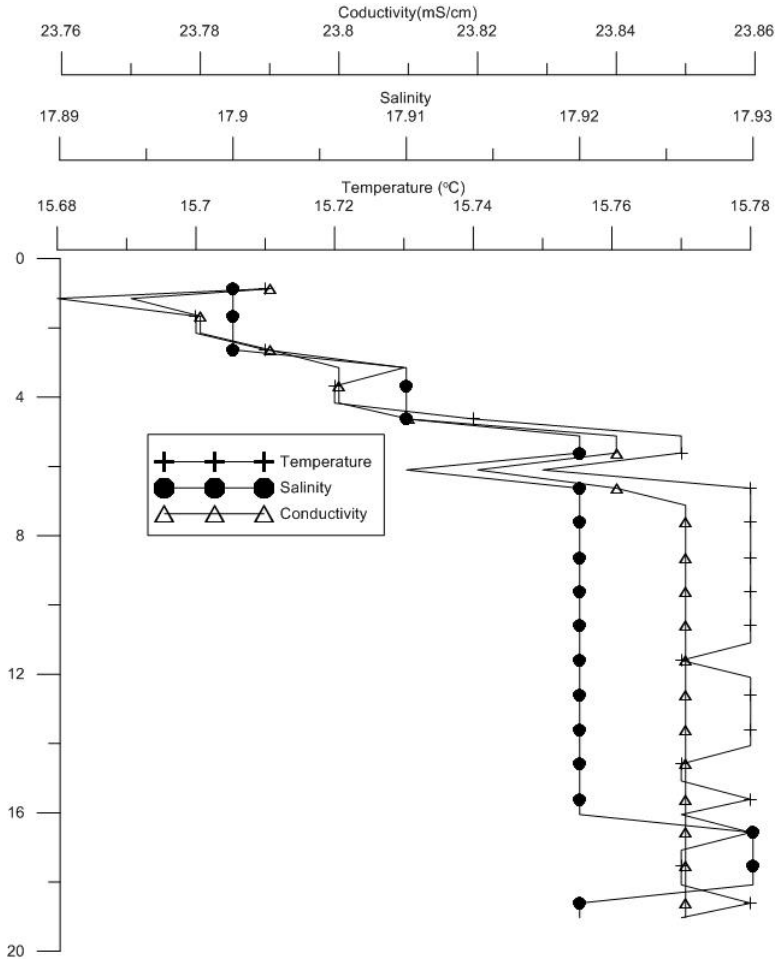

Figure 29: Sampling results of D5 station

4.3.3 Current Measurements and Modelling of Sürmene River

Current measurement results were given for surface measurements in Table 4: and Figure 30:.

Table 4: Current measurements for Sürmene River

	Month	time	Temp.	Pressure	Speed	Direction		
		hour	−C	dbar	m/s	degrees	Latitude	Longitude
1	07 18 2021	10 04 00	24,9	0.395	0,957	241,8	40°55'02,71"	40°06'35,97"
2	07 18 2021	10 14 05	25,43	0.438	0,324	252,01	40°54'58,39"	40°06' 50,51"
3	07 18 2021	10 20 00	25,92	1.014	0,482	248,6	40°55'10.71"	40°06'42.88"
4	07 18 2021	10 25 30	26,5	0.501	0,767	253,34	40°55'07.55"	40°06'59.76"
5	07 18 2021	10 40 45	26,87	0.479	0,55	339,55	40°55'04.85"	40°07'23.74"

Figure 30: Current measurents at Surmene coast

Wind speed of 19 knots and 8 different wind directions are used to simulate coastal currents of Sürmene Coast. These are N, NE,S,SE,W,NW,SW,E. All simulations were run for a day. Then, amount of litter were reduced by 10%, 30% and 70%, in order to see their effects. Results of these simulations are as follows:

4.3.4 Wind Directions of Turkish Coastal Area

4.3.4.1 Wind Direction: North (N)

The following figure shows the simulation results of North wind conditions after a day (Figure 31:)

Figure 31: Result of North wind condition for Surmene River

Then, litters were reduced 10%, 30% and 70%. The results of these simulations are given in Figure 32:.

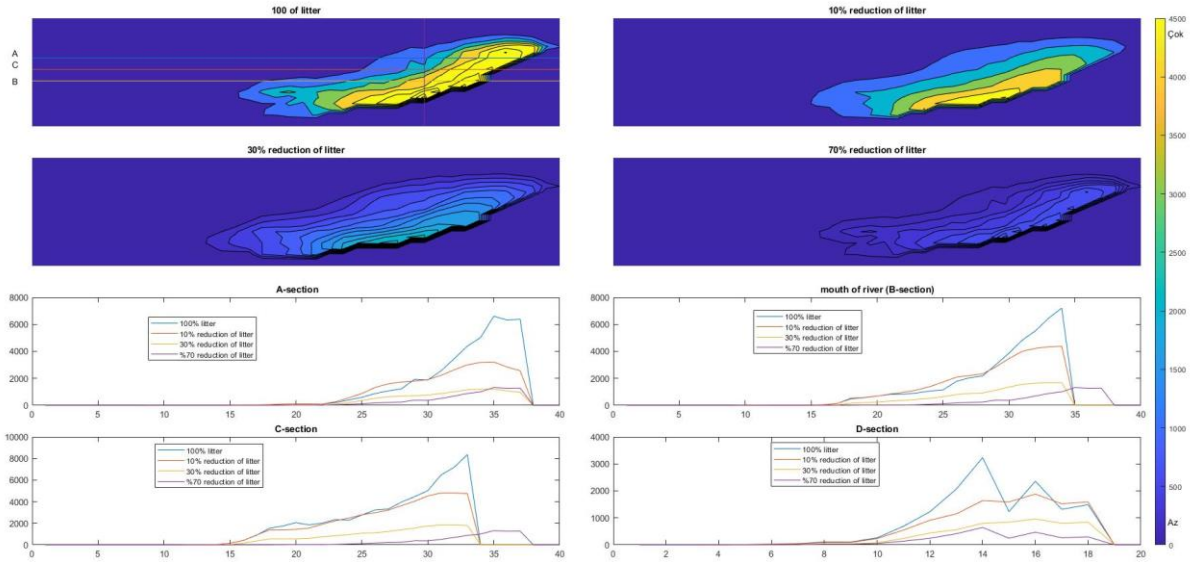

Figure 32: Litter distributions after %10, %30 and 70%reductions with N wind direction

4.3.4.2 Wind Direction: North-East (NE)

The following figure shows the simulation results of Northeast wind conditions after a day (Figure 33:)

Figure 33: Result of Northeast wind condition for Surmene River

Then, litters were reduced 10%, 30% and 70%. The results of these simulations are given in Figure 34:.

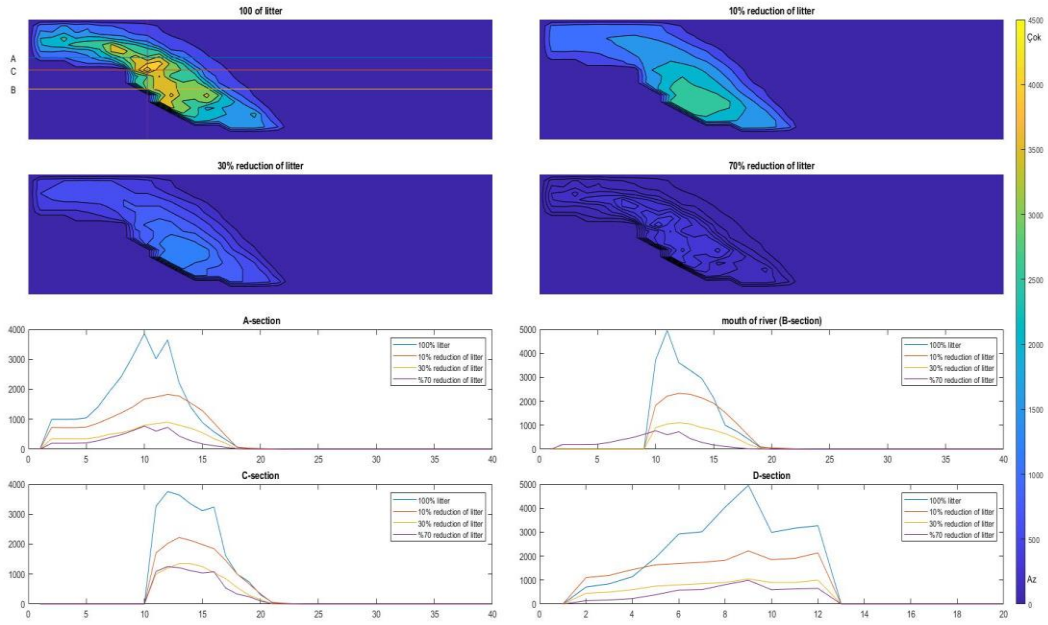

Figure 34: Litter distributions after %10, %30 and 70%reductions with NE wind direction

4.3.4.3 Wind Direction: East (E)

The following figure shows the simulation results of East wind conditions after a day (Figure 35:).

Figure 35: Result of East wind condition for Surmene River

Then, litters were reduced 10%, 30% and 70%. The results of these simulations are given in Figure 36:.

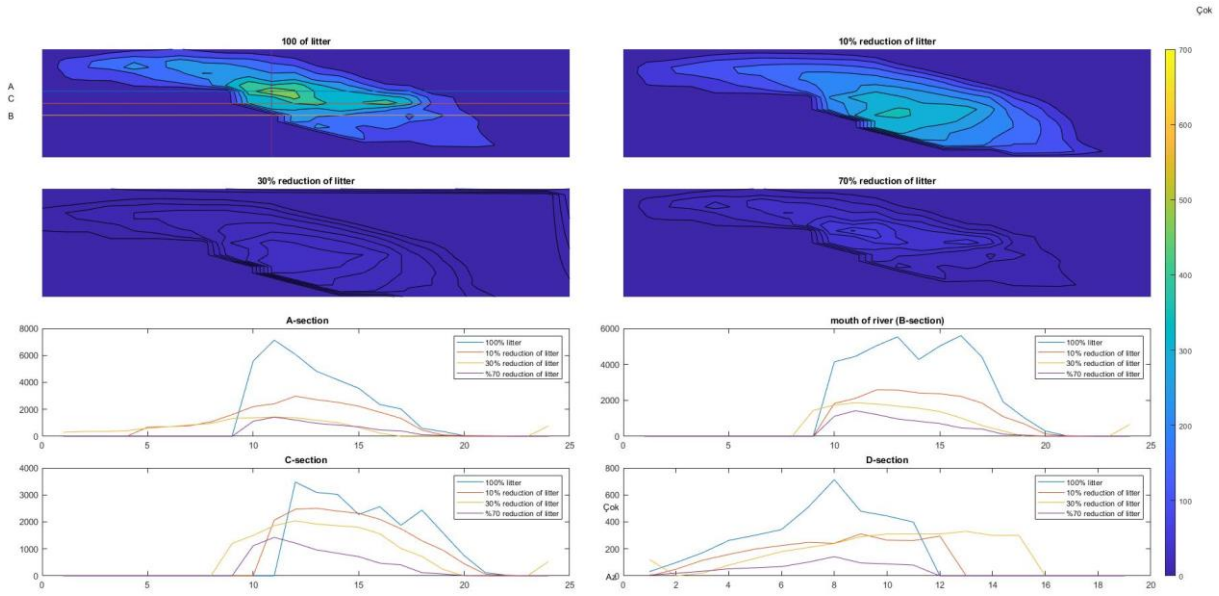

Figure 36: Litter distributions after %10, %30 and 70%reductions with E wind direction

4.3.4.4 Wind Direction: South-East (SE)

The following figure shows the simulation results of South-East wind conditions after a day (Figure 37:).

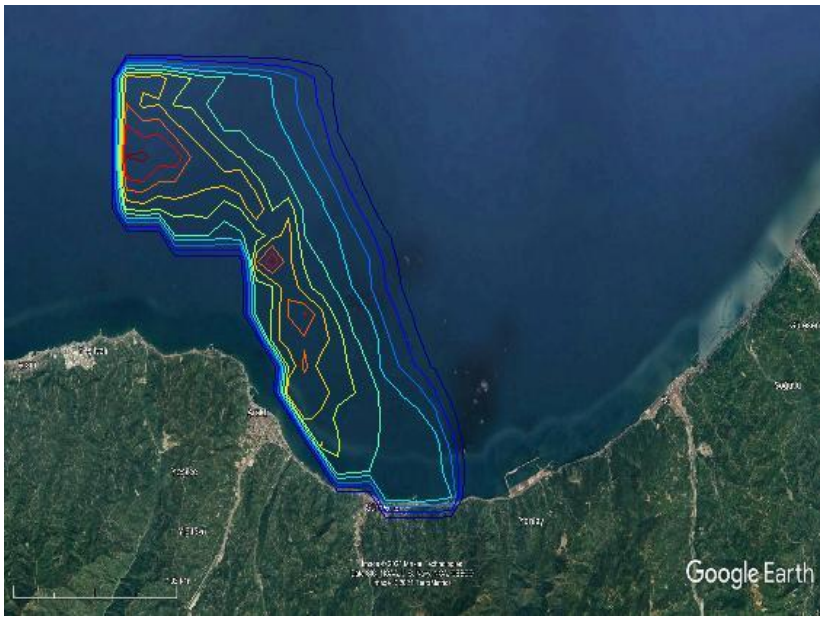

Figure 37: Result of Southeast wind condition for Surmene River

Then, litters were reduced 10%, 30% and 70%. The results of these simulations are given in Figure 38:.

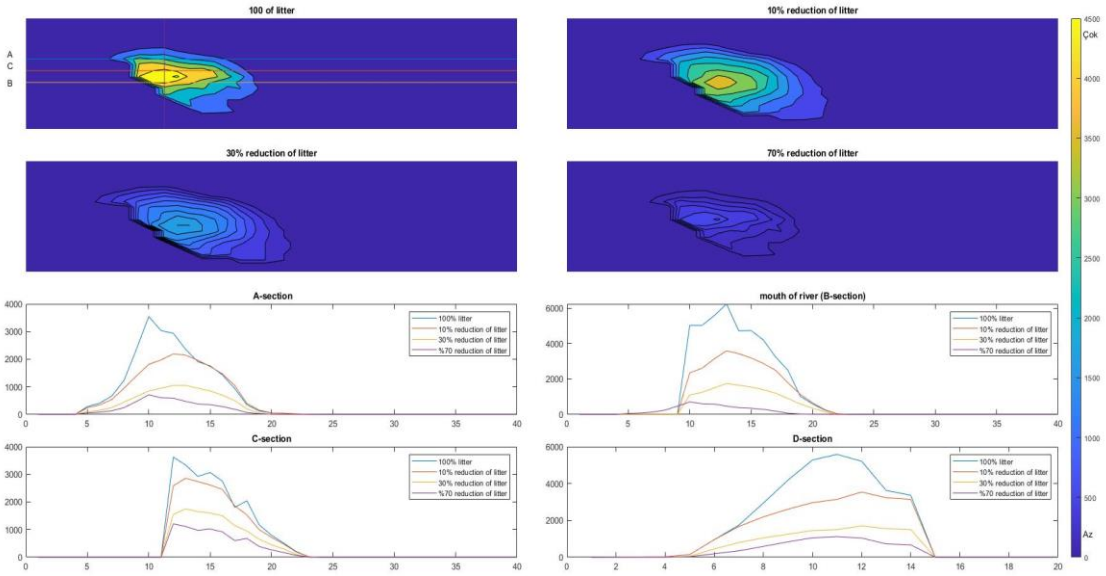

Figure 38: Litter distributions after %10, %30 and 70%reductions with SE wind direction

4.3.4.5 Wind Direction: South (S)

The following figure shows the simulation results of South wind conditions after a day (Figure 39:).

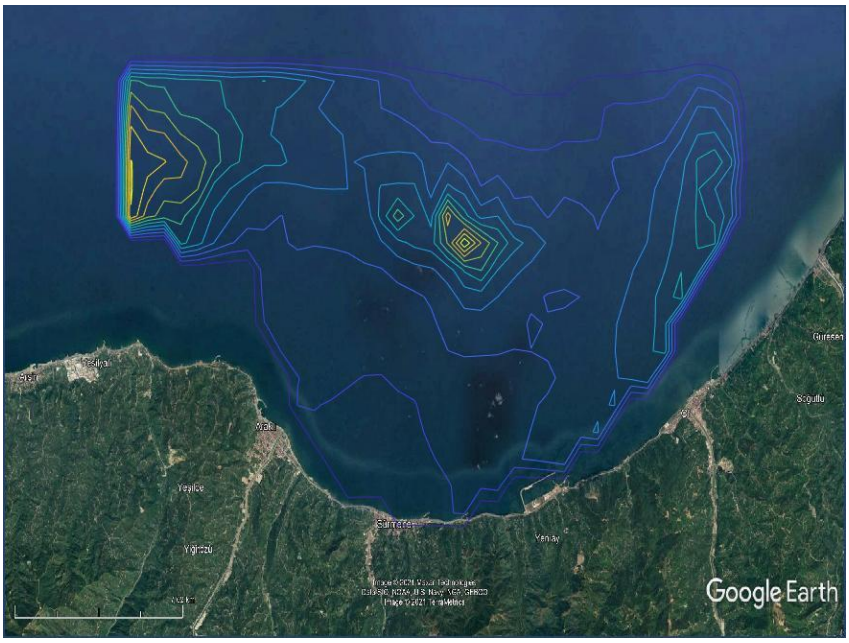

Figure 39: Result of South wind condition for Surmene River

Then, litters were reduced 10%, 30% and 70%. The results of these simulations are given in Figure 41:.

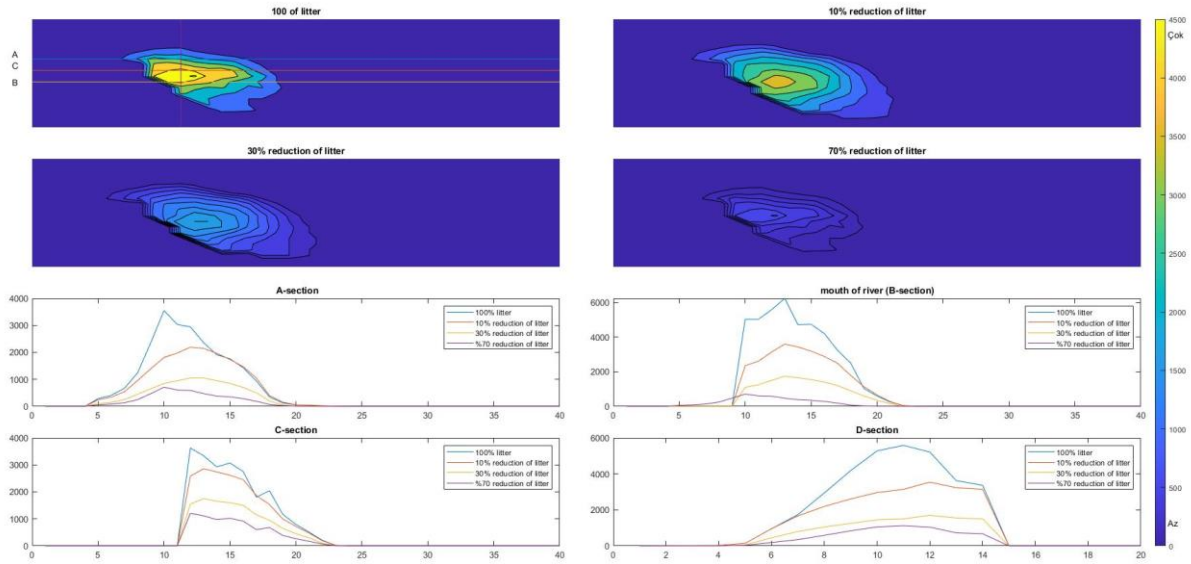

Figure 40: Litter distributions after %10, %30 and 70%reductions with SE wind direction

4.3.4.6 *Wi*nd Direction: South-West (SW)

The following figure shows the simulation results of South-west wind conditions after two days (Figure 41:)

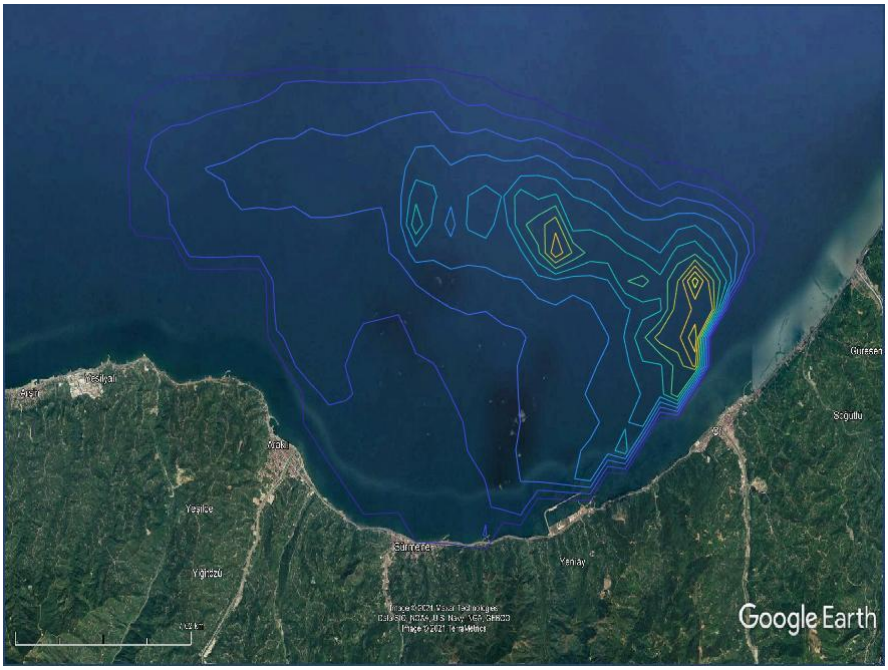

Figure 41: Result of Southwest wind condition for Surmene River

Then, litters were reduced 10%, 30% and 70%. The results of these simulations are given in Figure 42: .

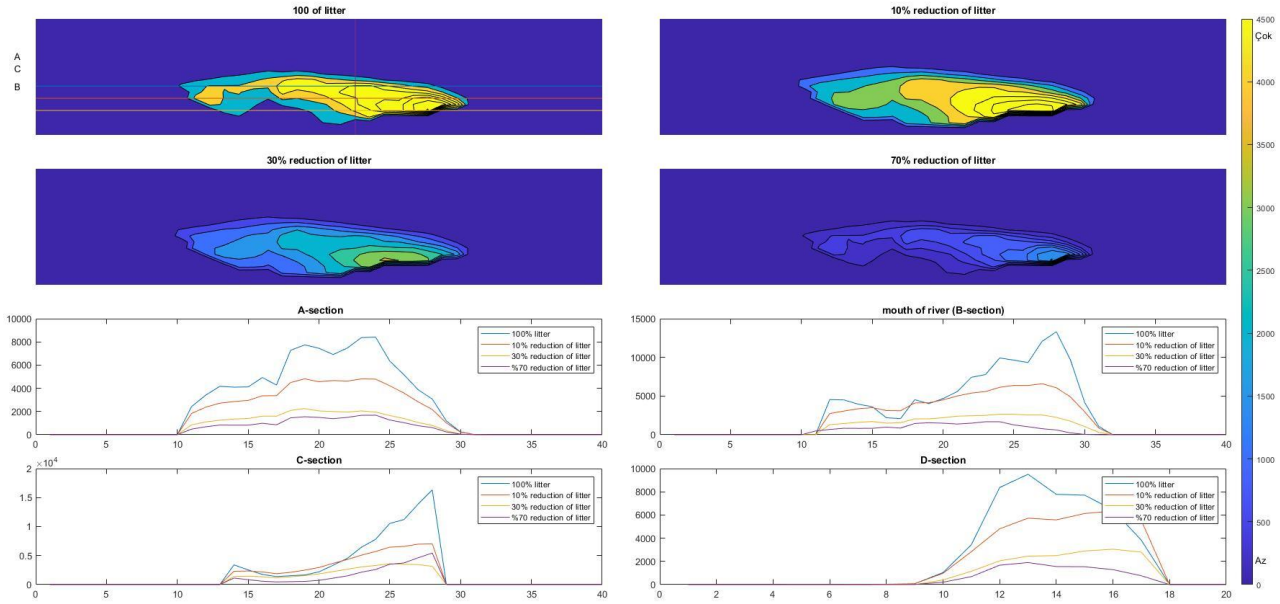

Figure 42: Litter distributions after %10, %30 and 70%reductions with SW wind direction

4.3.4.7 Wind Direction: West (W)

The following figure shows the simulation results of West wind conditions after a day (Figure 43:).

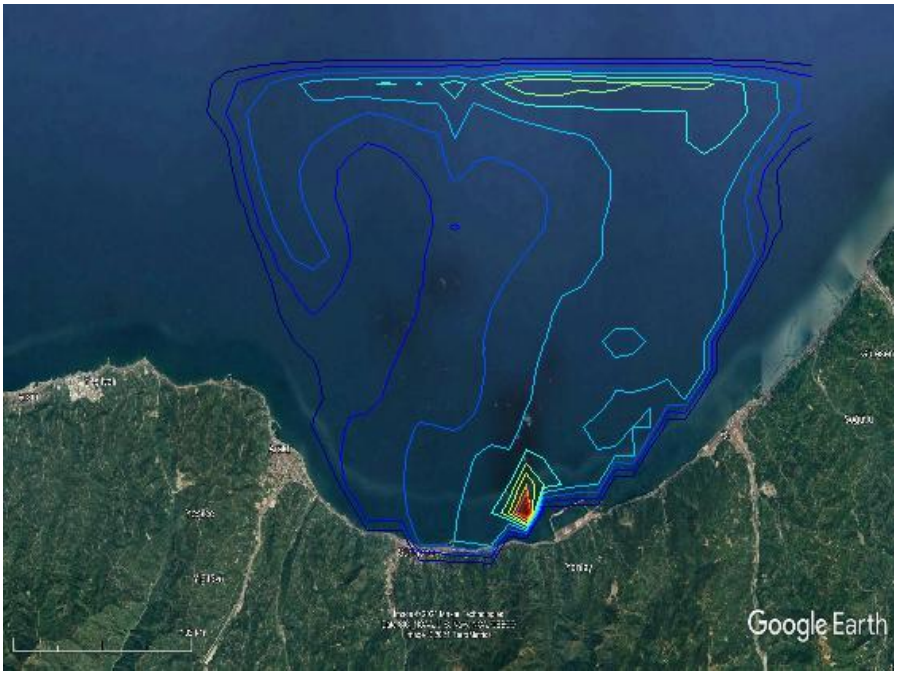

Figure 43: Result of west wind condition for Surmene River

Then, litters were reduced 10%, 30% and 70%. The results of these simulations are given in Figure 44:.

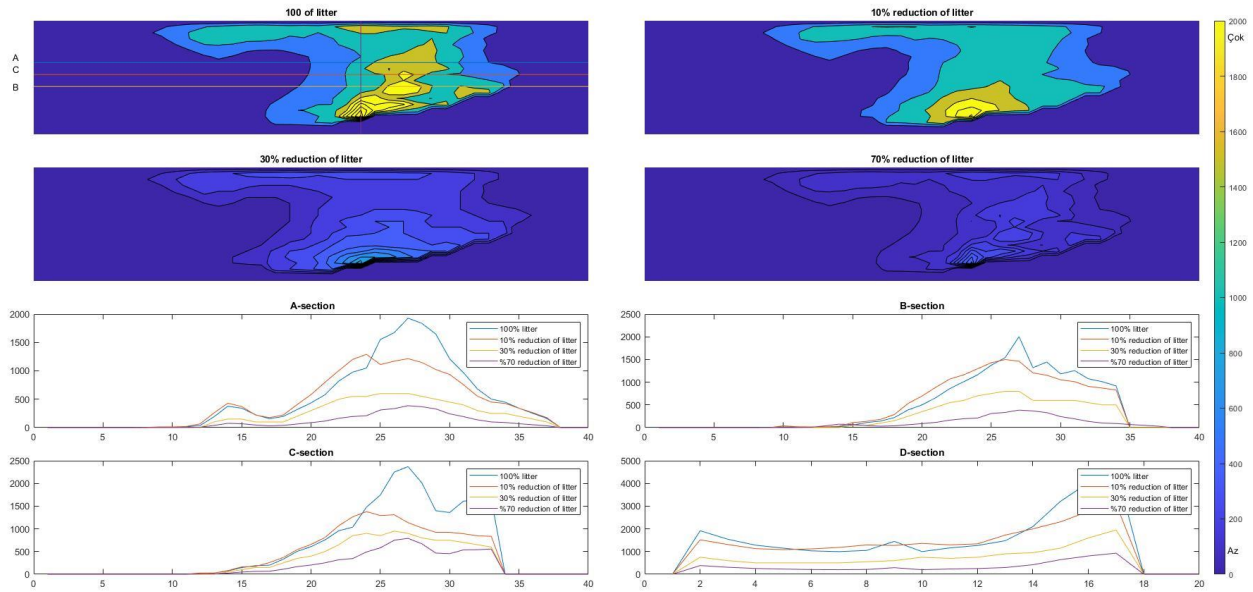

Figure 44: Litter distributions after %10, %30 and 70%reductions with SW wind direction

4.3.4.8 Wind Direction: North-West (NW)

The following figure shows the simulation results of Nort-west wind conditions after a day (Figure 45:).

Figure 45: Result of Northwest wind condition for Surmene River

Then, litters were reduced 10%, 30% and 70%. The results of these simulations are given in Figure 46.

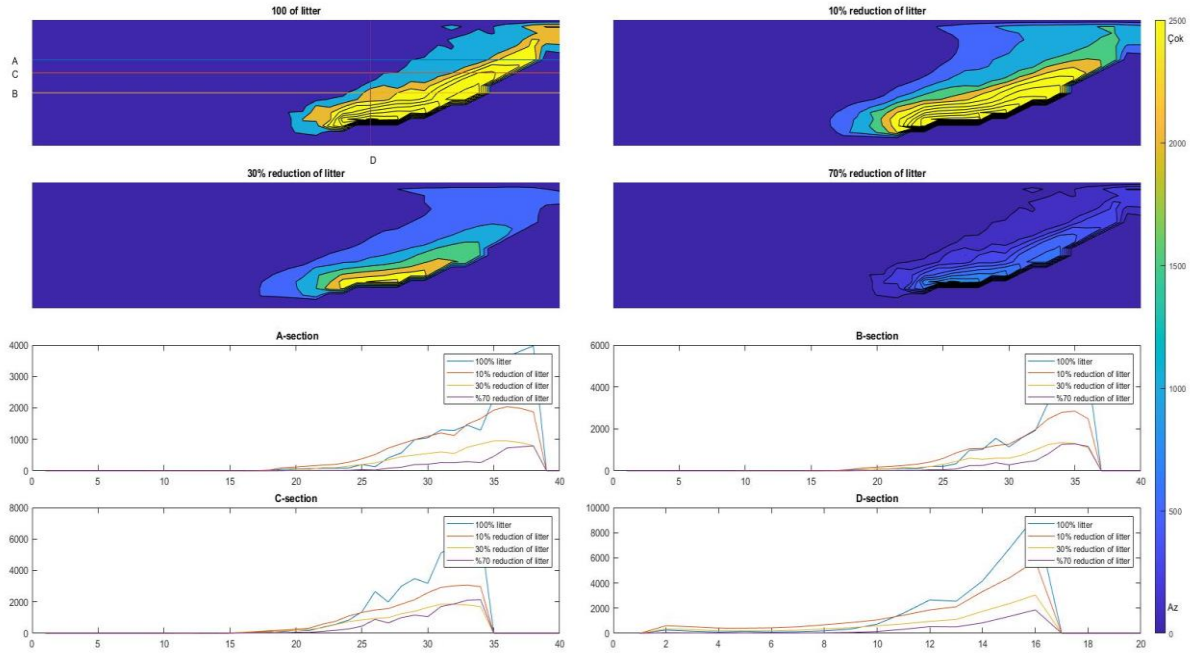

Figure 46: Litter distributions after %10, %30 and 70%reductions with NW wind direction

4.4 Simulations of Kamchia River

In order to simulate coastal currents, topography of the area has to be input in the POM. Therefore, topography of the Kamchia coast was taken from [6]

4.4.1 Topography of Kamchia River

3-D and contour graphics of topography of Kamchia River is given Figure 47.

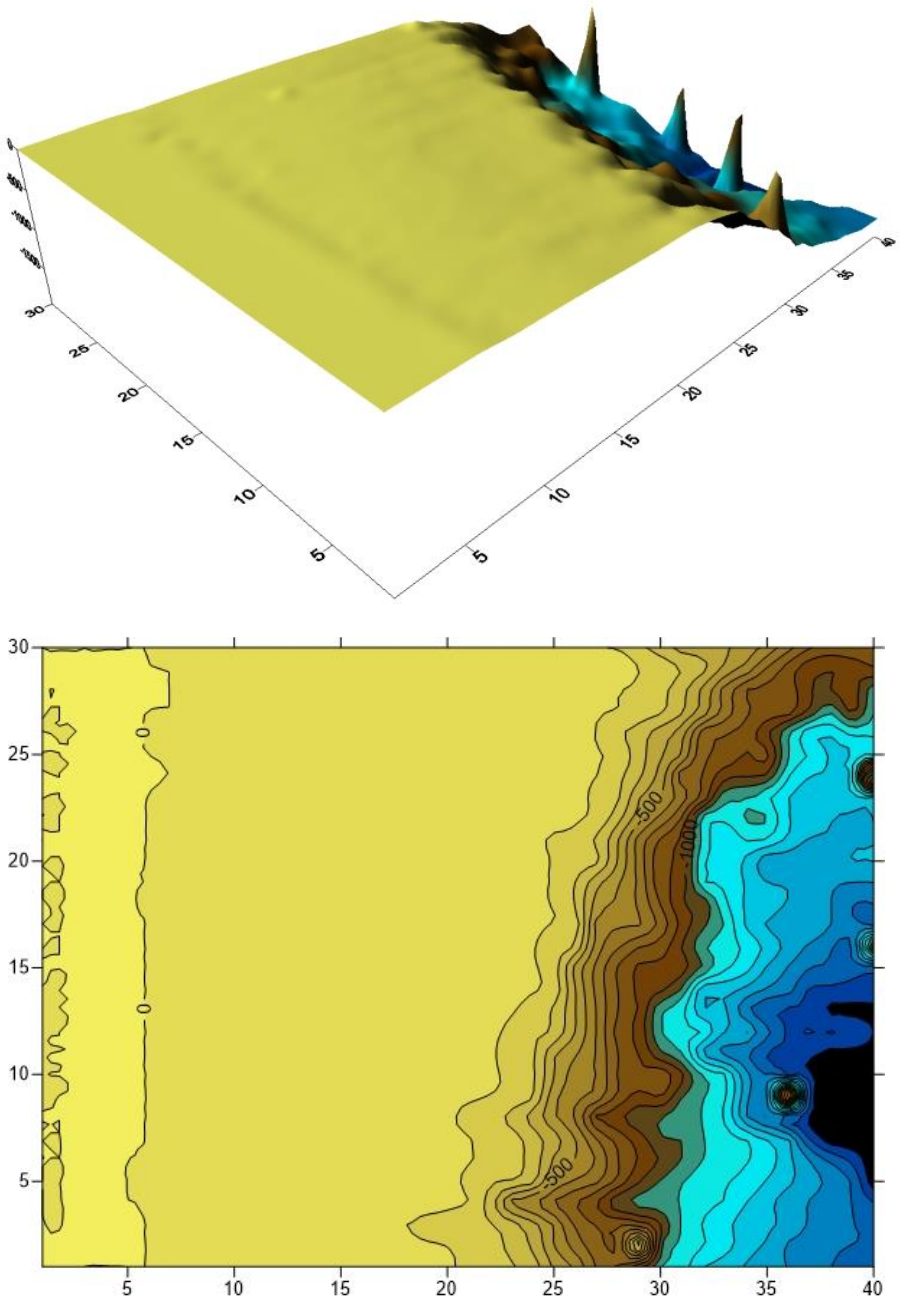

Figure 47: 3D and contour graphic (a) and Topography (b) of Kamchia River front

4.4.2 Wind Directions Of Bulgarian Coastal Area

4.4.2.1 Wind Direction: North (N)

The following figure shows the simulation results of North wind conditions after a day (Figure 48).

Figure 48: Result of North wind condition for Kamchia River

Then, litters were reduced 10%, 30% and 70%. The results of these simulations are given in Figure 49Figure 32:.

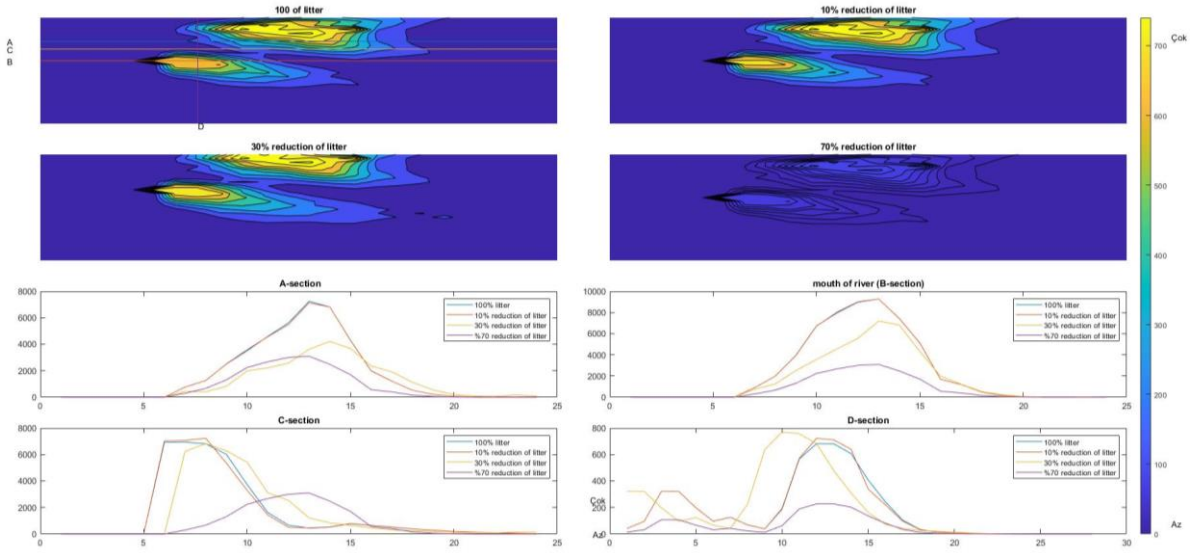

Figure 49: Litter distributions after %10, %30 and 70%reductions with N wind direction

4.4.2.2 *W*ind Direction: North-East (NE)

The following figure shows the simulation results of North-East wind conditions after a day (Figure 50).

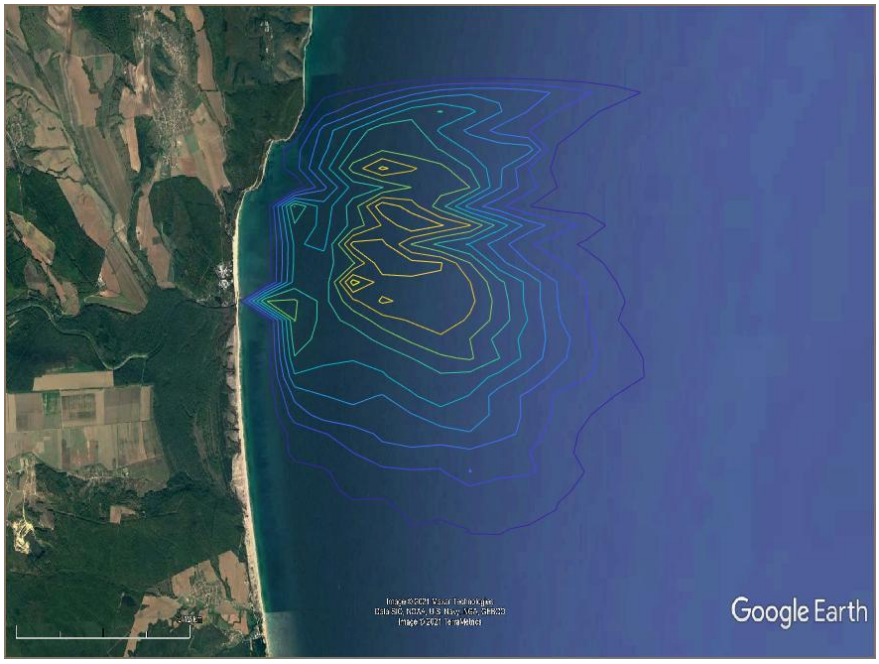

Figure 50: Result of Northeast wind condition for Kamchia River

Then, litters were reduced 10%, 30% and 70%. The results of these simulations are given in Figure 51.

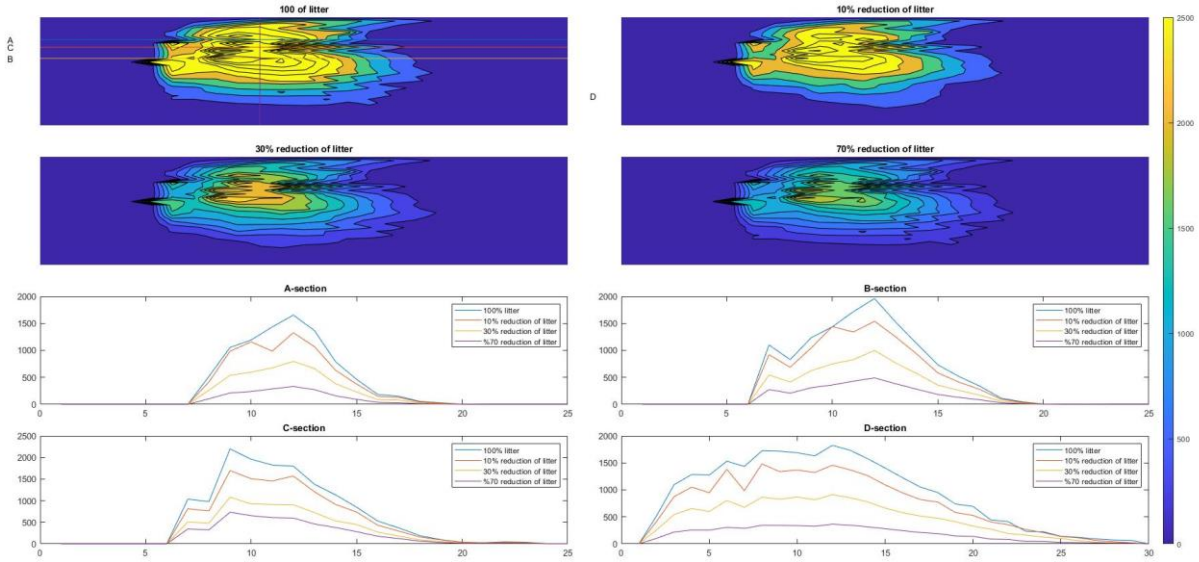

Figure 51: Litter distributions after %10, %30 and 70%reductions with NE wind direction

4.4.2.3 Wind Direction: East (E)

The following figure shows the simulation results of East wind conditions after a day(Figure 52).

Figure 52: Result of East wind condition for Kamchia River

Then, litters were reduced 10%, 30% and 70%. The results of these simulations are given in Figure 53.

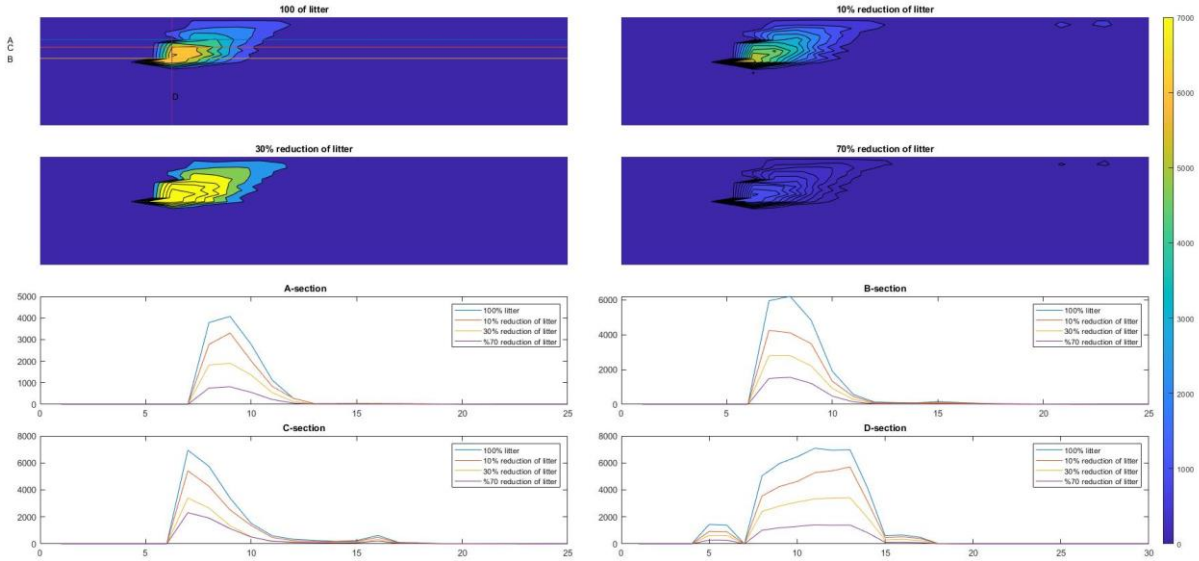

Figure 53: Litter distributions after %10, %30 and 70%reductions with E wind direction

4.4.2.4 Wind Direction: South-East (SE)

The following figure shows the simulation results of South-East wind conditions after a day (Figure 54).

Figure 54: Result of Southeast wind condition for Kamchia River

Then, litters were reduced 10%, 30% and 70%. The results of these simulations are given in Figure 55.

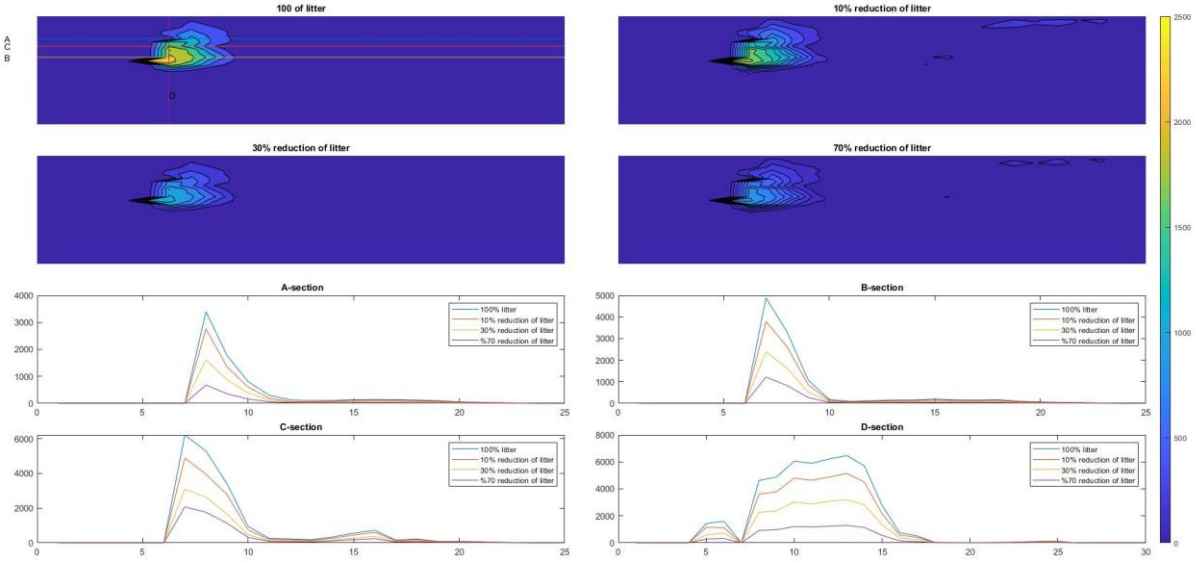

Figure 55: Litter distributions after %10, %30 and 70%reductions with SE wind direction

4.4.2.5 Wind Direction: South (S)

The following figure shows the simulation results of South wind conditions after a day (Figure 39:Figure 56**).**

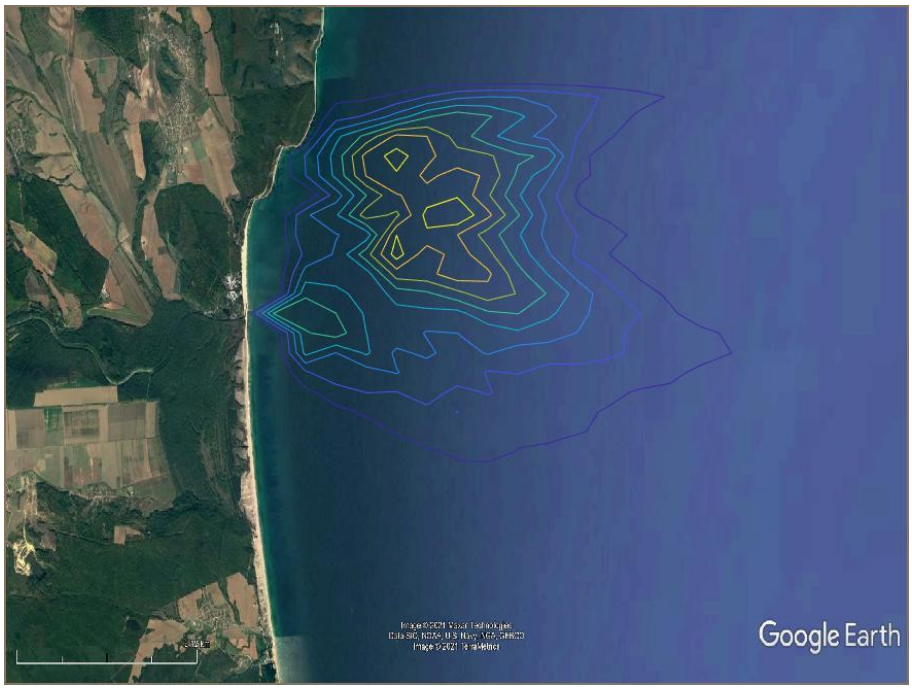

Figure 56: Result of South wind condition for Kamchia River

Then, litters were reduced 10%, 30% and 70%. The results of these simulations are given in Figure 41:.

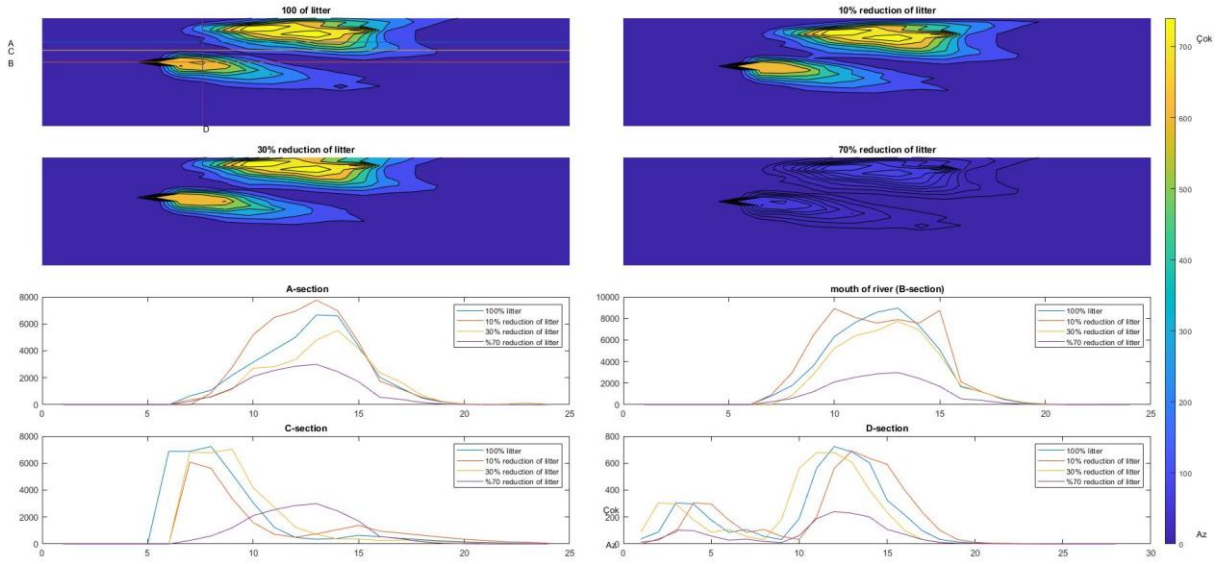

Figure 57: Litter distributions after %10, %30 and 70%reductions with SE wind direction

4.4.2.6 Wind Direction: South-West (SW)

The following figure shows the simulation results of South-West wind conditions after two days (Figure 58).

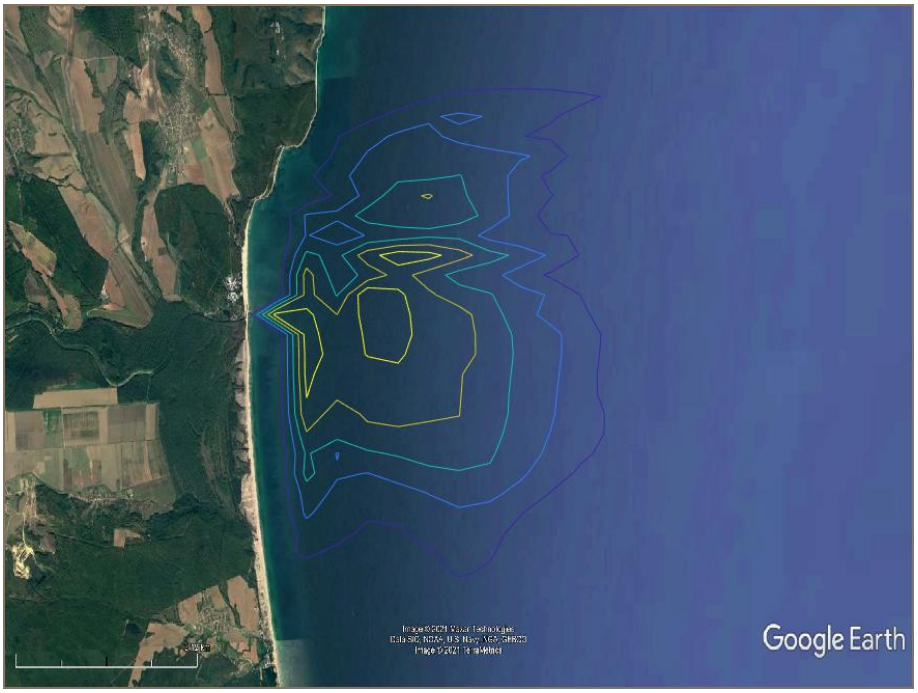

Figure 58: Result of Southwest wind condition for Kamchia River

Then, litters were reduced 10%, 30% and 70%. The results of these simulations are given in 59 .

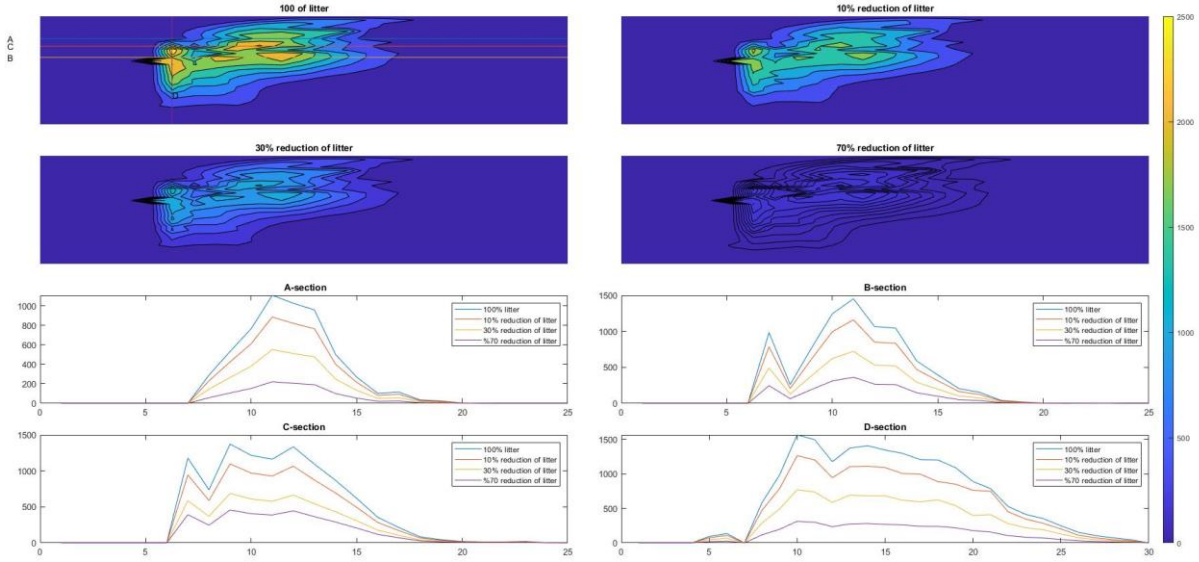

Figure 59: Litter distributions after %10, %30 and 70%reductions with SW wind direction

4.4.2.7 Wind Direction: West (W)

The following figure shows the simulation results of West wind conditions after a day (Figure 60).

Figure 60: Result of west wind condition for Kamchia River

Then, litters were reduced 10%, 30% and 70%. The results of these simulations are given in Figure 61Figure 44:.

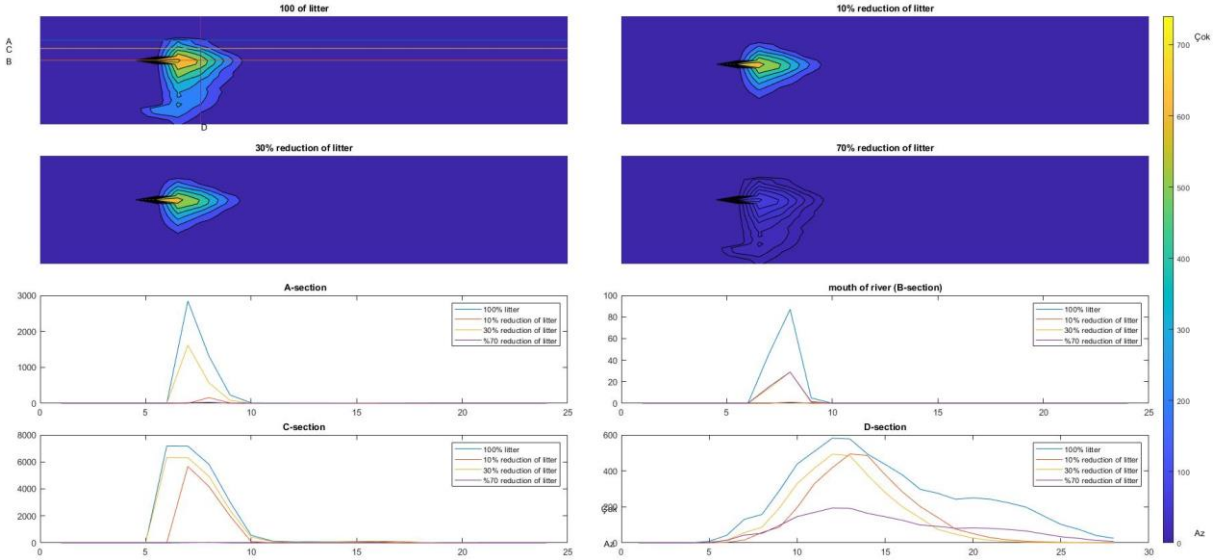

Figure 61: Litter distributions after %10, %30 and 70%reductions with SW wind direction

4.4.2.8 Wind Direction: North-West (NW)

The following figure shows the simulation results of North-West wind conditions after a day (Figure 62).

Figure 62: Result of Northwest wind condition for Kamchia River

Then, litters were reduced 10%, 30% and 70%. The results of these simulations are given in Figure 63.

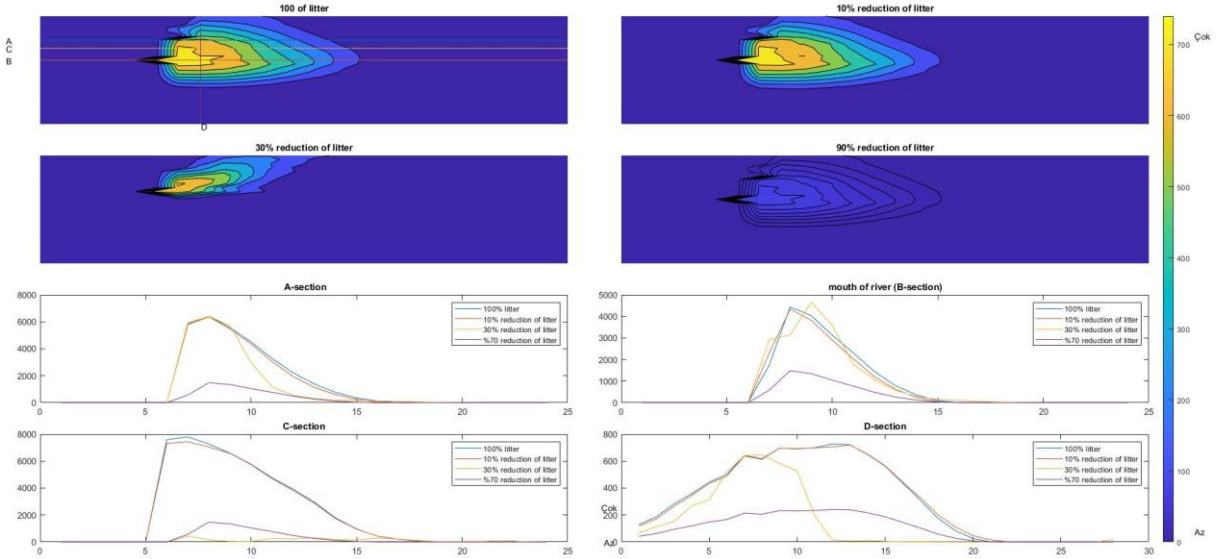

Figure 63: Litter distributions after %10, %30 and 70%reductions with NW wind direction

4.5 Simulations of Danube River

In order to simulate coastal currents, topography of the area has to be input in the POM. Therefore, topography of the Danube coast was taken from [6]

4.5.1 Topography of Danube River

3-D and contour graphics of topography of Danube River is given Figure 64.

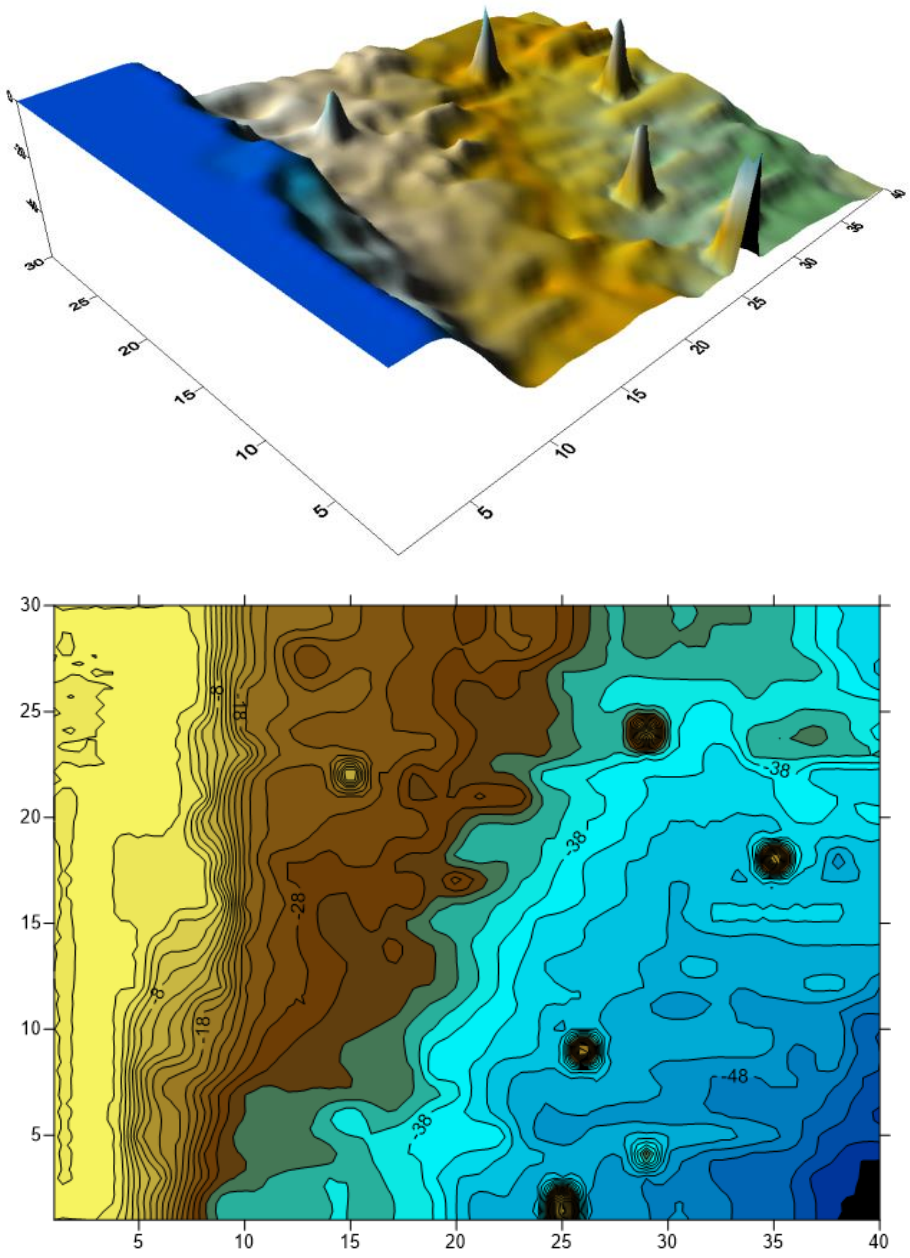

Figure 64: 3D and contour graphic (a) and Topography (b) of Danube River front

4.5.2 Wind Directions Of Romanian Coastal Area

4.5.2.1 Wind Direction: North (N)

The following figure shows the simulation results of North wind conditions after a day (Figure 65).

Figure 65: Result of North wind condition for Danube River

Then, litters were reduced 10%, 30% and 70%. The results of these simulations are given in Figure 66Figure 32:.

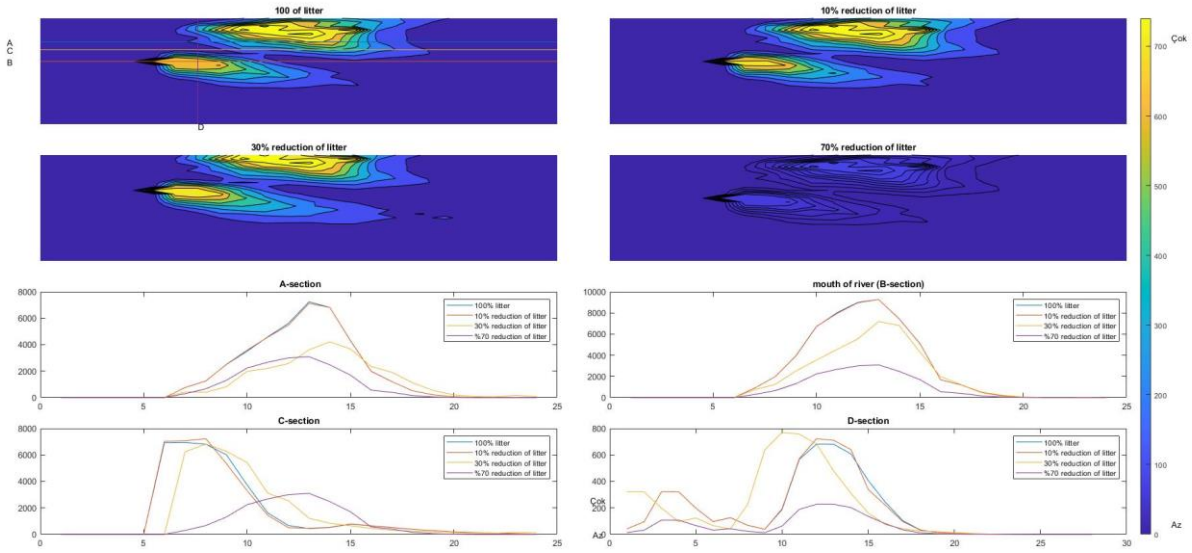

Figure 66: Litter distributions after %10, %30 and 70%reductions with N wind direction

4.5.2.2 *W*ind Direction: North-East (NE)

The following figure shows the simulation results of North-East wind conditions after a day (Figure 67).

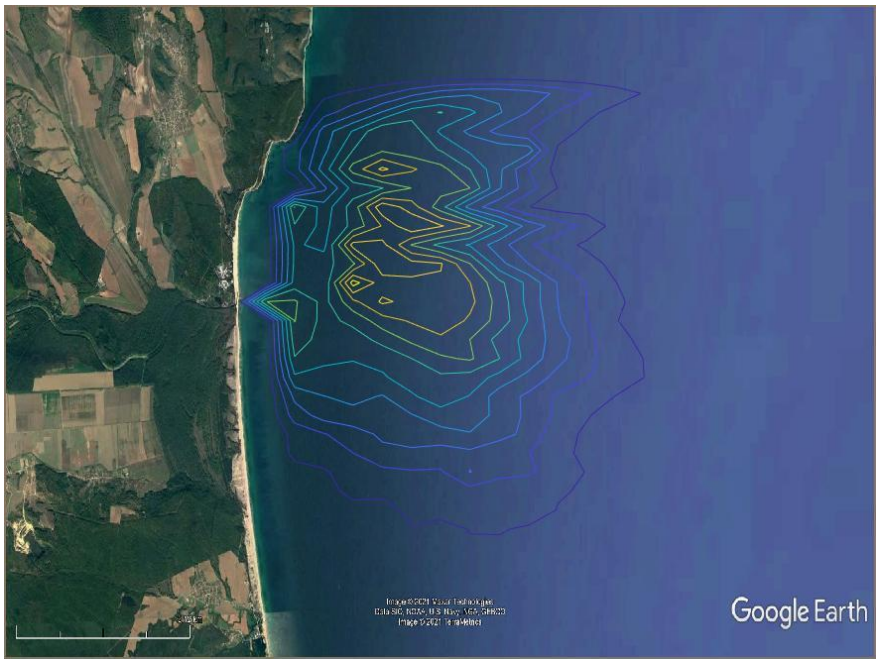

Figure 67: Result of Northeast wind condition for Danube River

Then, litters were reduced 10%, 30% and 70%. The results of these simulations are given in Figure 68Figure 34:.

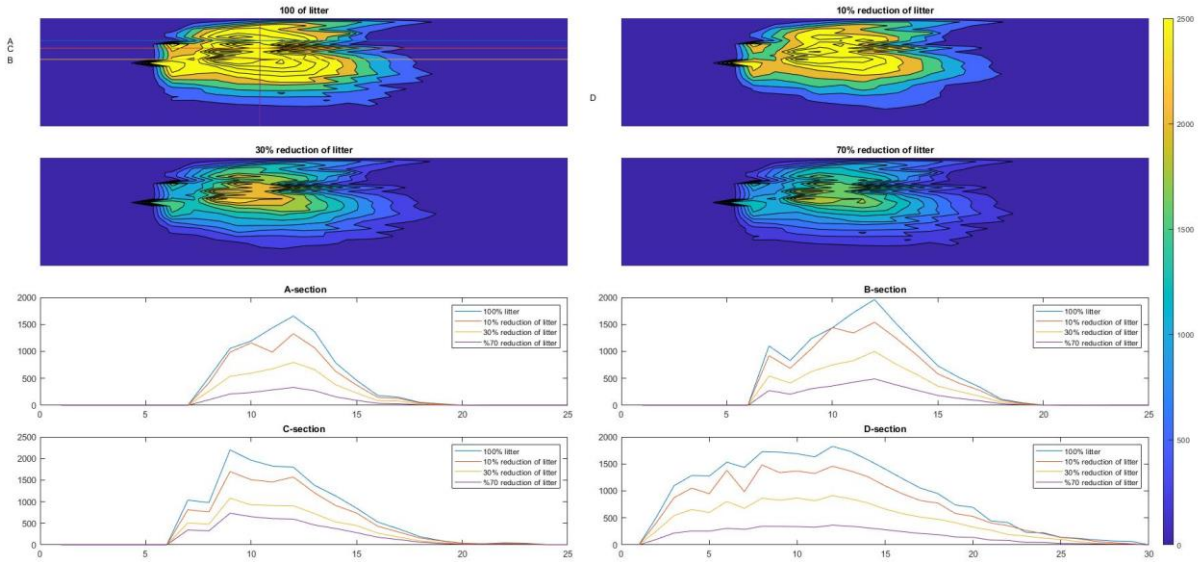

Figure 68: Litter distributions after %10, %30 and 70%reductions with NE wind direction

4.5.2.3 Wind Direction: East (E)

The following figure shows the simulation results of East wind conditions after a day (Figure 69Figure 35:).

Figure 69: Result of East wind condition for Danube River

Then, litters were reduced 10%, 30% and 70%. The results of these simulations are given in Figure 70.

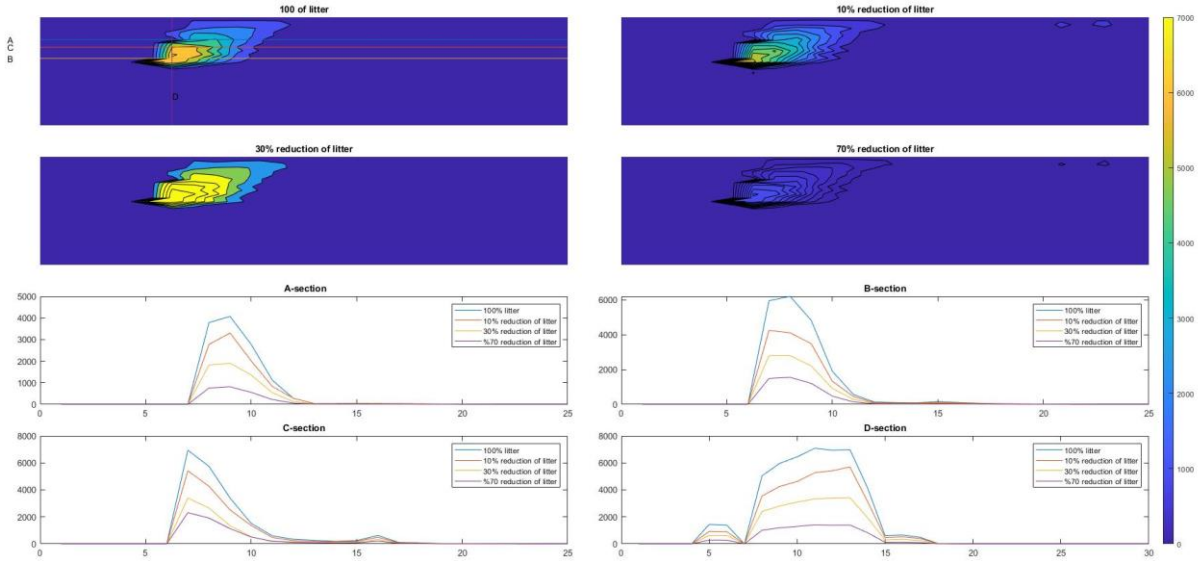

Figure 70: Litter distributions after %10, %30 and 70%reductions with E wind direction

4.5.2.4 Wind Direction: South-East (SE)

The following figure shows the simulation results of South-East wind conditions after a day (Figure 71).

Figure 71: Result of Southeast wind condition for Danube River

Then, litters were reduced 10%, 30% and 70%. The results of these simulations are given in Figure 72Figure 38:.

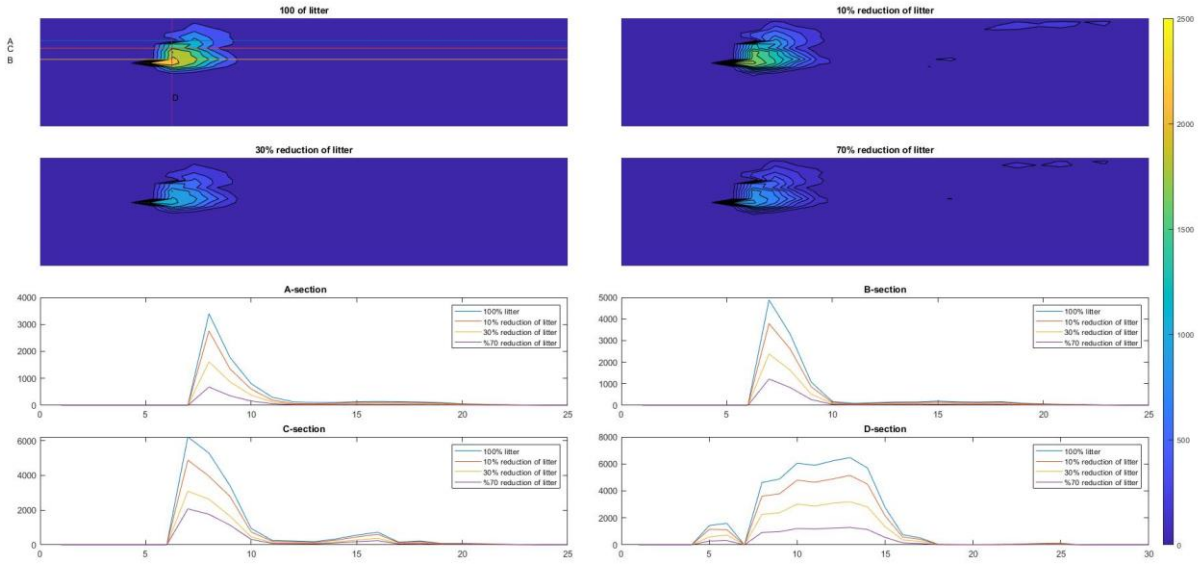

Figure 72: Litter distributions after %10, %30 and 70%reductions with SE wind direction

4.5.2.5 Wind Direction: South (S)

The following figure shows the simulation results of South wind conditions after a day (Figure 39:Figure 73).

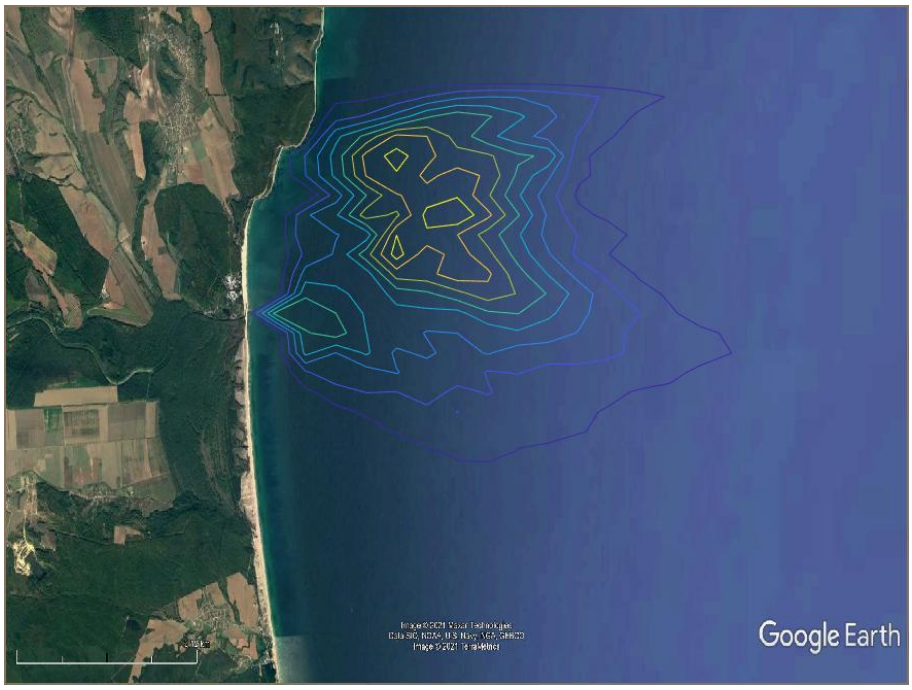

Figure 73: Result of South wind condition for Danube River

Then, litters were reduced 10%, 30% and 70%. The results of these simulations are given in Figure 74.

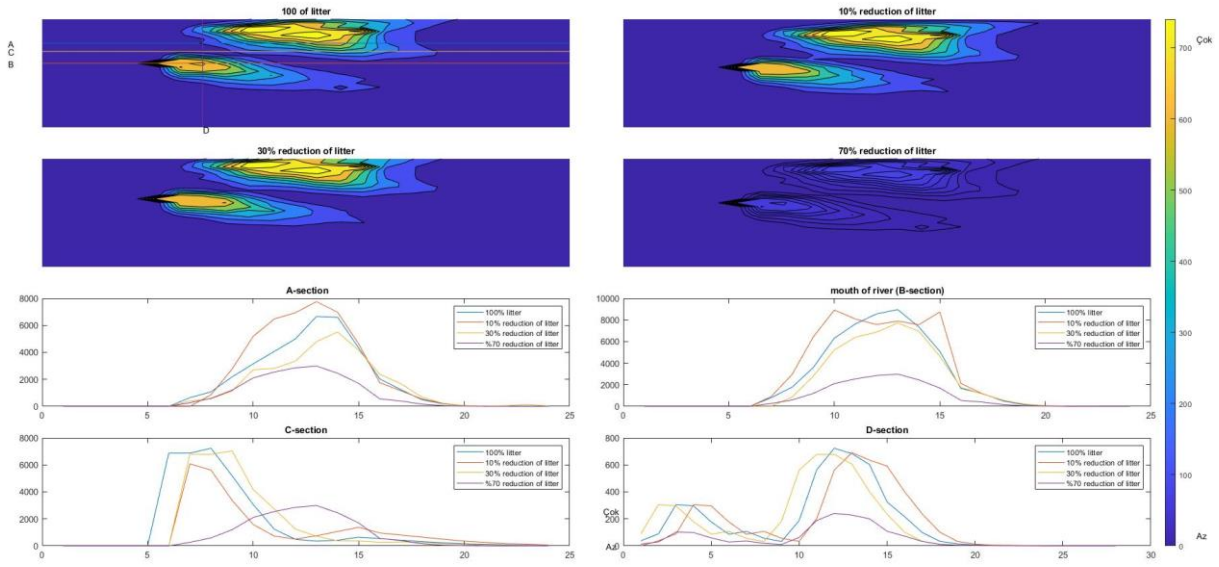

Figure 74: Litter distributions after %10, %30 and 70%reductions with SE wind direction

4.5.2.6 Wind Direction: South-West (SW)

The following figure shows the simulation results of South-West wind conditions after two days (Figure 75).

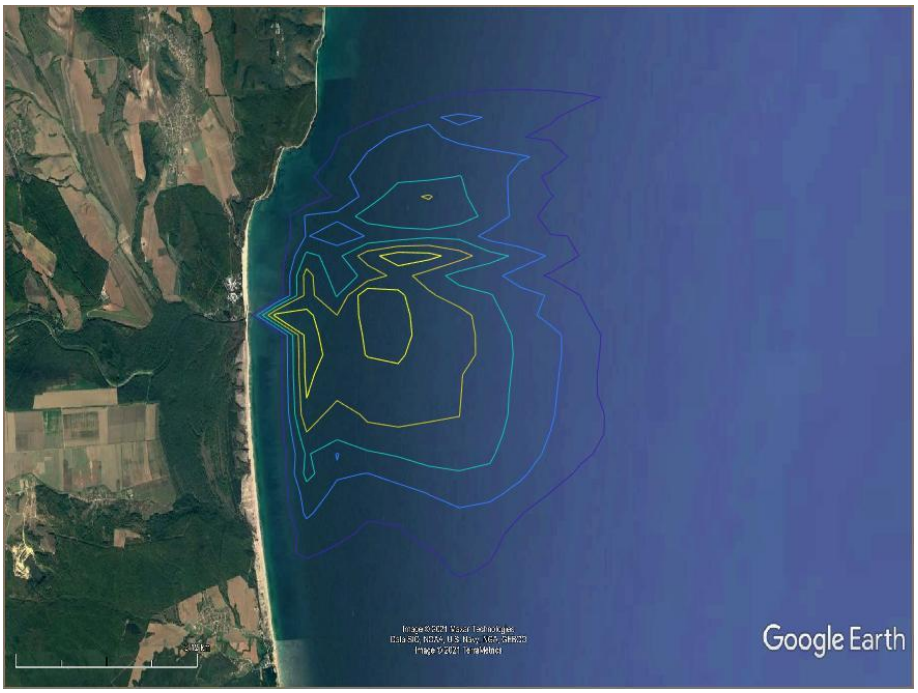

Figure 75: Result of Southwest wind condition for Danube River

Then, litters were reduced 10%, 30% and 70%. The results of these simulations are given in Figure 76 .

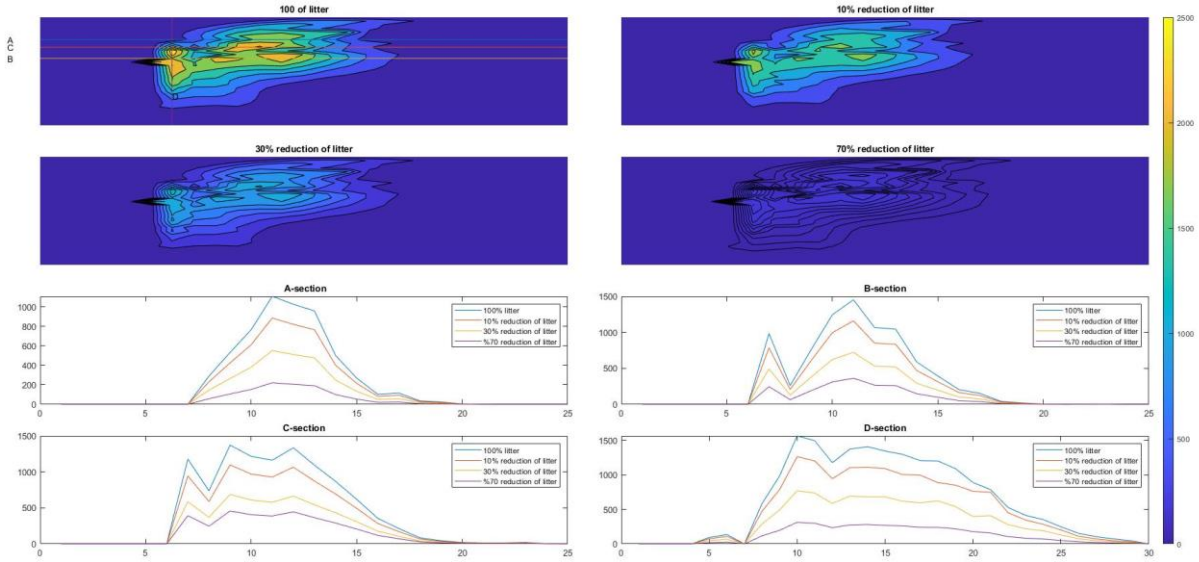

Figure 76: Litter distributions after %10, %30 and 70%reductions with SW wind direction

4.5.2.7 Wind Direction: West (W)

The following figure shows the simulation results of West wind conditions after a day (Figure 77).

Figure 77: Result of west wind condition for Danube River

Then, litters were reduced 10%, 30% and 70%. The results of these simulations are given in Figure 78.

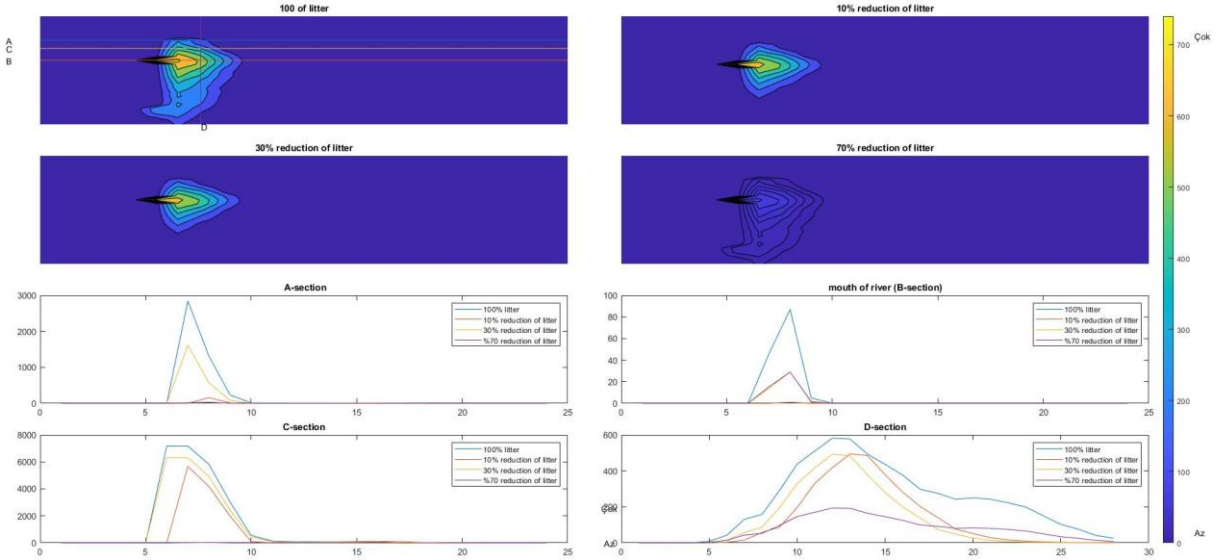

Figure 78: Litter distributions after %10, %30 and 70%reductions with SW wind direction

4.5.2.8 Wind Direction: North-West (NW)

The following figure shows the simulation results of North-West wind conditions after a day (Figure 79).

Figure 79: Result of Northwest wind condition for Danube River

Then, litters were reduced 10%, 30% and 70%. The results of these simulations are given in Figure 80.

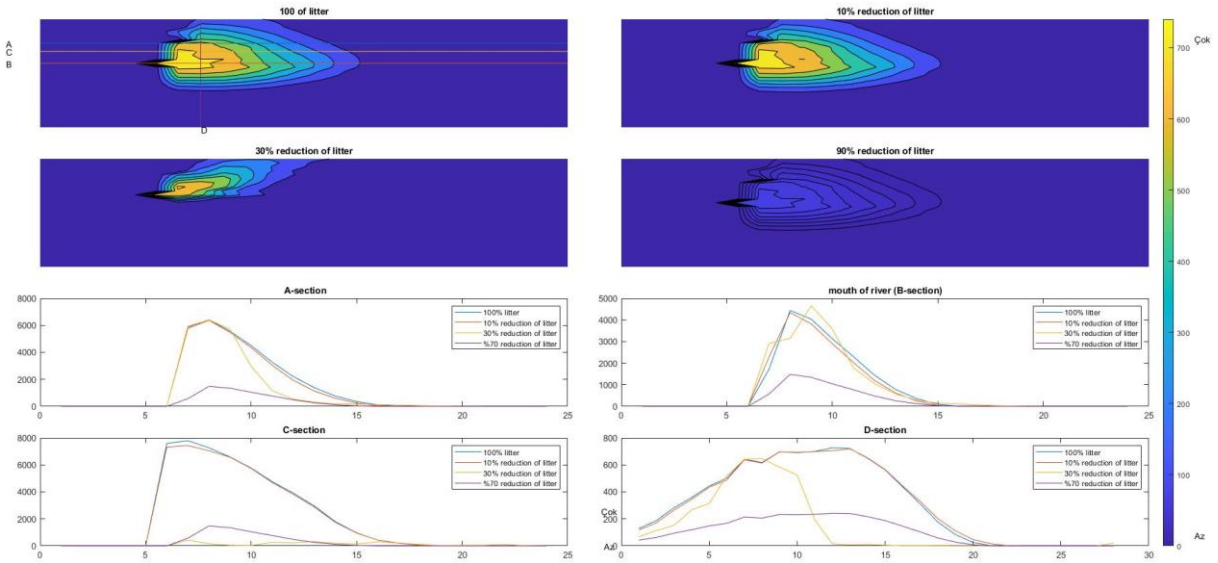

Figure 80: Litter distributions after %10, %30 and 70%reductions with NW wind direction

4.6 Simulations of Choruhi River

In order to simulate coastal currents, topography of the area has to be input in the POM. Therefore, topography of the Chouruhi coast was taken from [6]

4.6.1 Topography of Choruhi River

3-D and contour graphics of topography of Danube River is givenFigure 81.

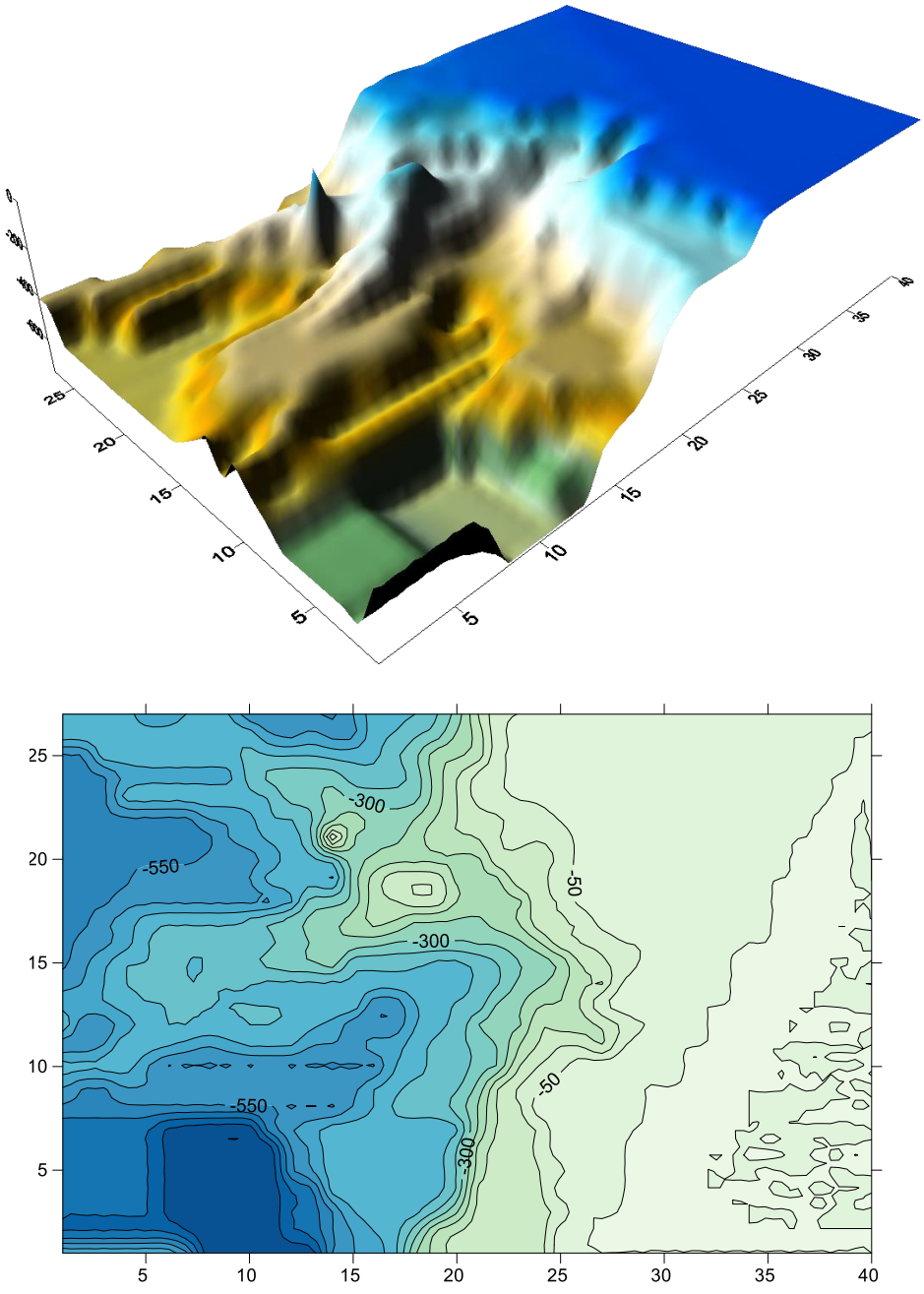

Figure 81: 3D and contour graphic (a) and Topography (b) of Choruhi River front

4.6.2 Wind Directions Of Georgian Coastal Area

4.6.2.1 Wind Direction: North (N)

The following figure shows the simulation results of North wind conditions after a day (Figure 82).

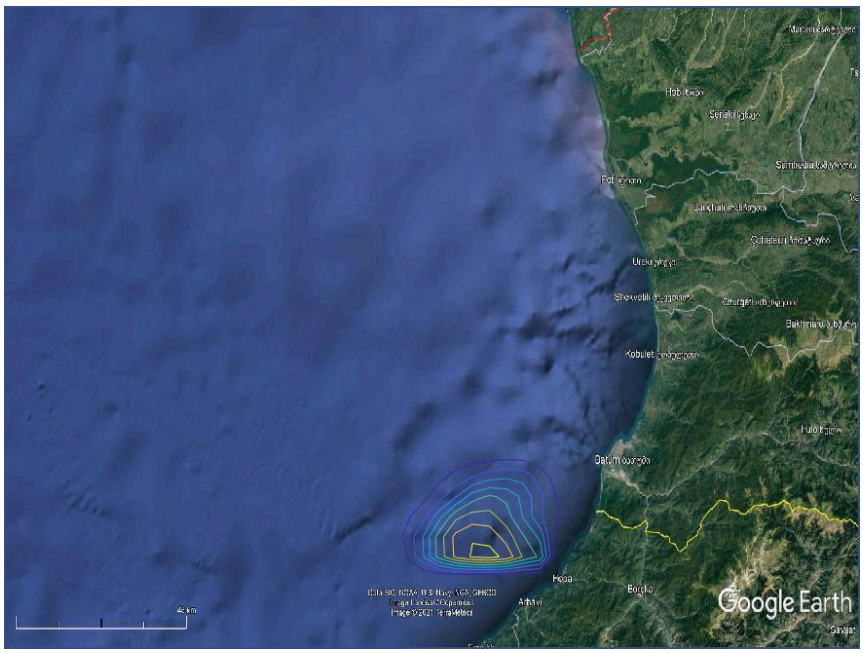

Figure 82: Result of North wind condition for Choruhi River

Then, litters were reduced 10%, 30% and 70%. The results of these simulations are given in Figure 66Figure 83Figure 32:.

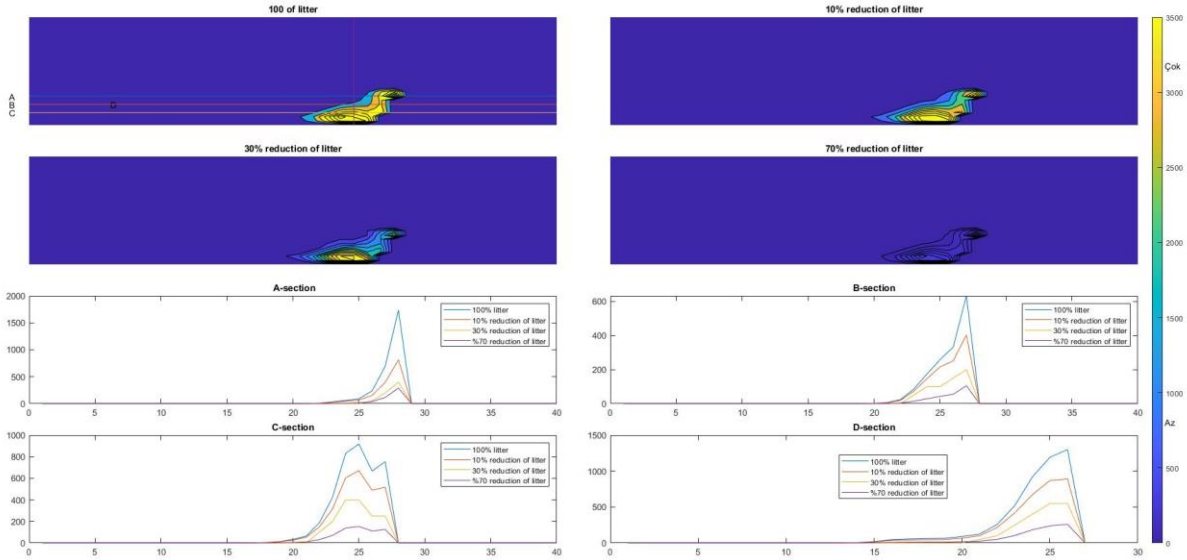

Figure 83: Litter distributions after %10, %30 and 70%reductions with N wind direction

4.6.2.2 *W*ind Direction: North-East (NE)

The following figure shows the simulation results of North-East wind conditions after a day (Figure 84).

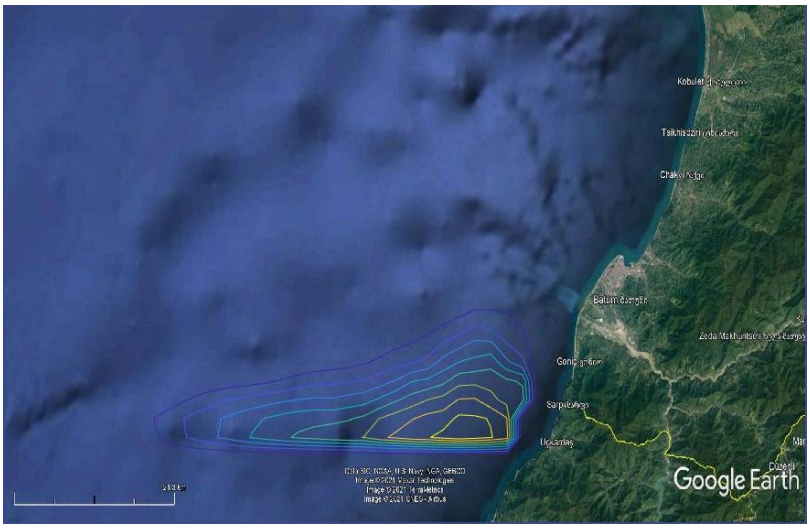

Figure 84: Result of Northeast wind condition for Choruhi River

Then, litters were reduced 10%, 30% and 70%. The results of these simulations are given in Figure 85Figure 68Figure 34:.

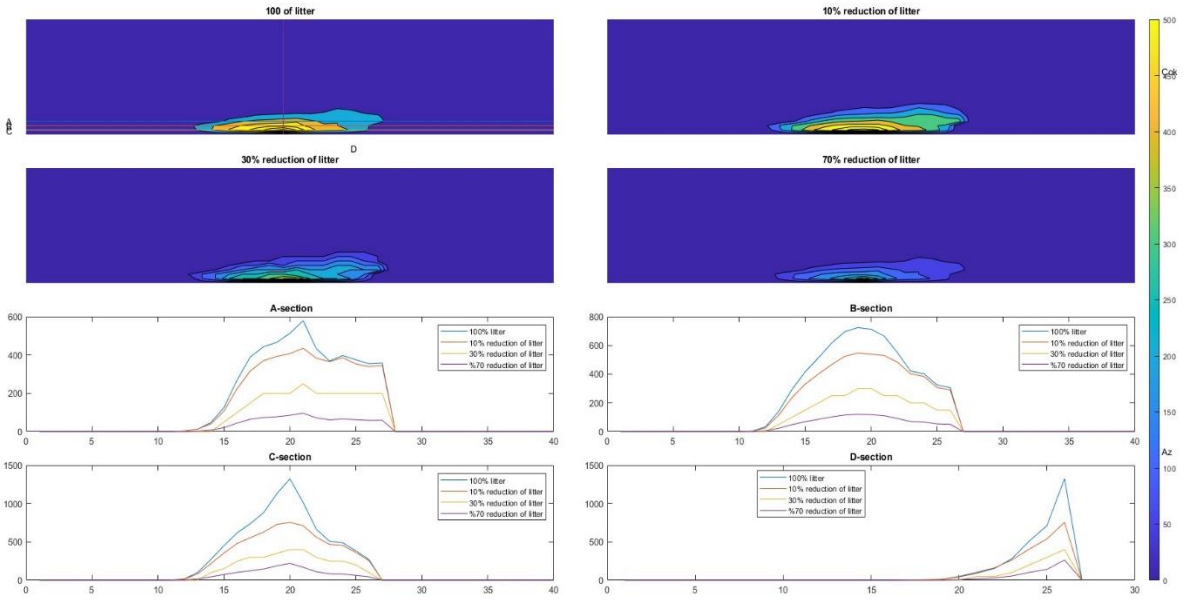

Figure 85: Litter distributions after %10, %30 and 70%reductions with NE wind direction

4.6.2.3 Wind Direction: East (E)

The following figure shows the simulation results of East wind conditions after a day (Figure 86Figure 35:).

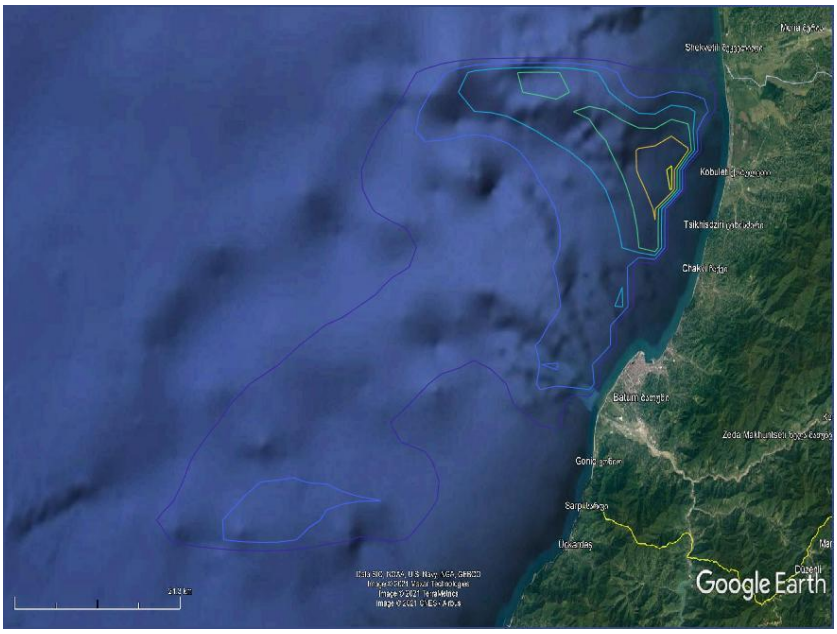

Figure 86: Result of East wind condition for Choruhi River

Then, litters were reduced 10%, 30% and 70%. The results of these simulations are given in Figure 87

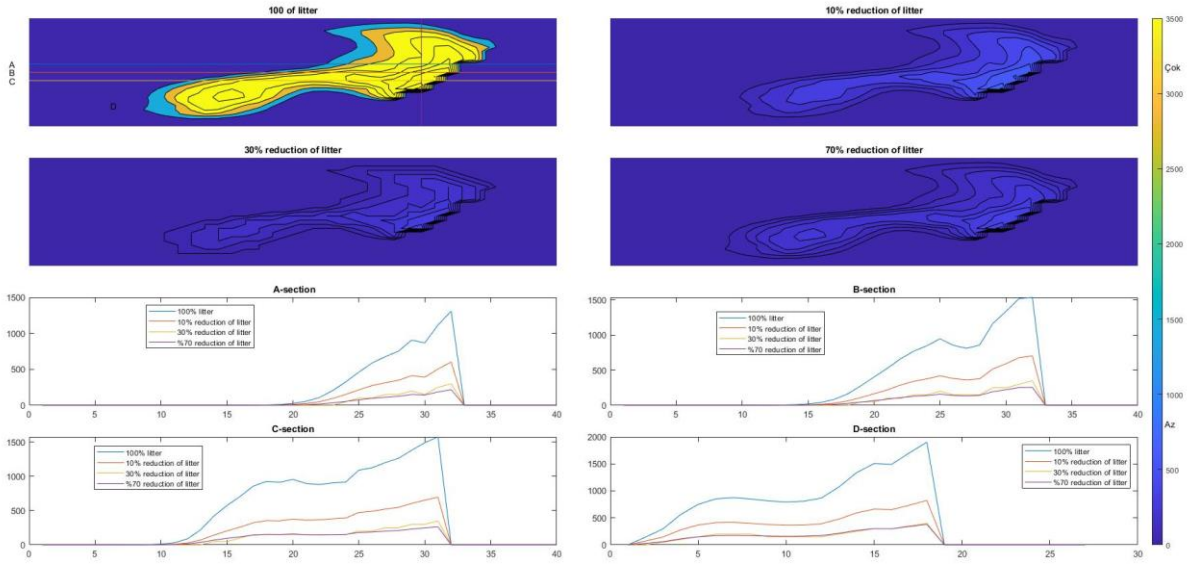

Figure 87: Litter distributions after %10, %30 and 70%reductions with E wind direction

4.6.2.4 Wind Direction: South-East (SE)

The following figure shows the simulation results of South-East wind conditions after a day (Figure 88).

Figure 88: Result of Southeast wind condition for Choruhi River

Then, litters were reduced 10%, 30% and 70%. The results of these simulations are given in Figure 89Figure 38:.

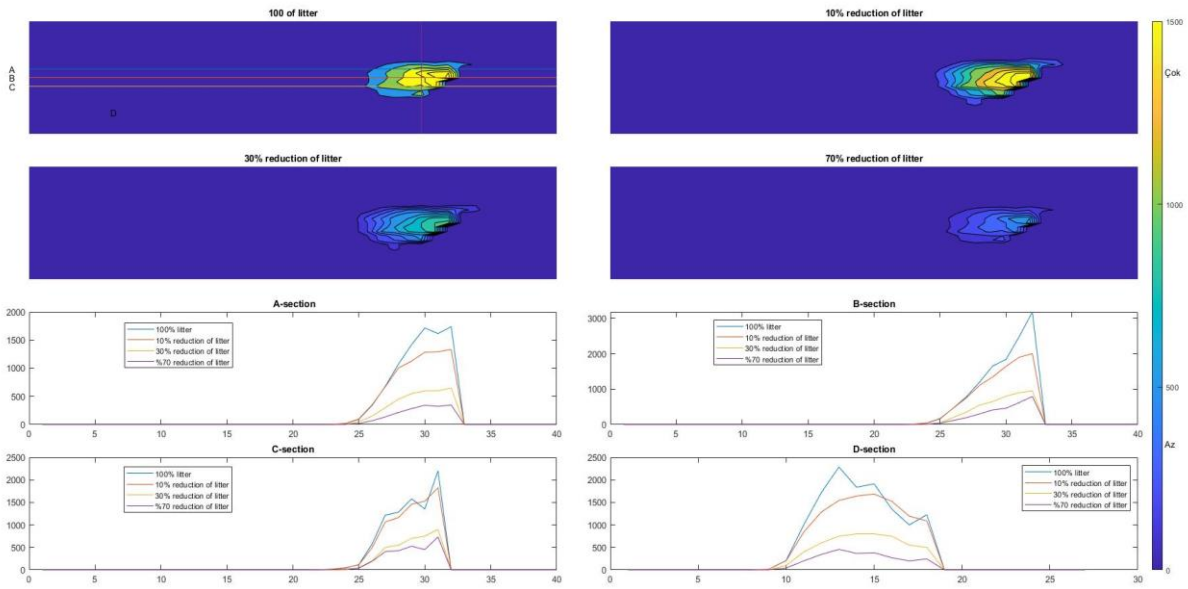

Figure 89: Litter distributions after %10, %30 and 70%reductions with SE wind direction

4.6.2.5 Wind Direction: South (S)

The following figure shows the simulation results of South wind conditions after a day (Figure 39:Figure 90).

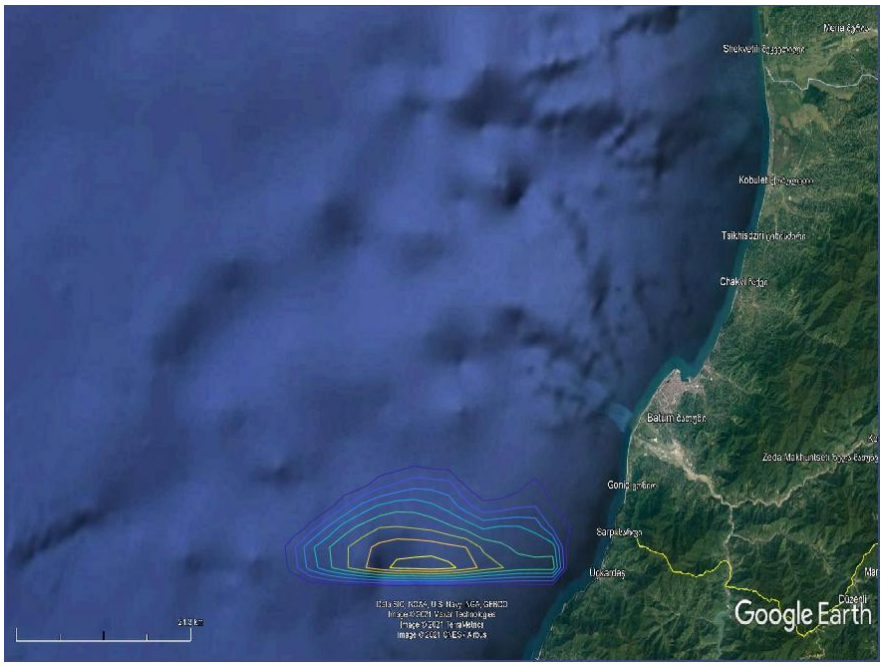

Figure 90: Result of South wind condition for Choruhi River

Then, litters were reduced 10%, 30% and 70%. The results of these simulations are given in Figure 91Figure 74.

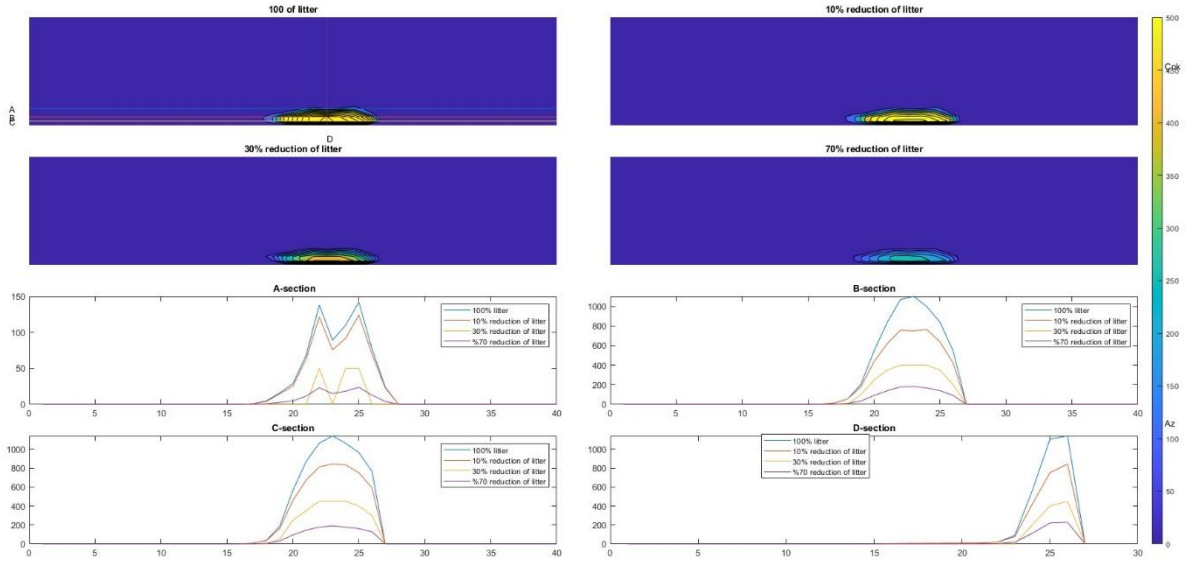

Figure 91: Litter distributions after %10, %30 and 70%reductions with SE wind direction

4.6.2.6 Wind Direction: South-West (SW)

The following figure shows the simulation results of South-West wind conditions after two days (Figure 92).

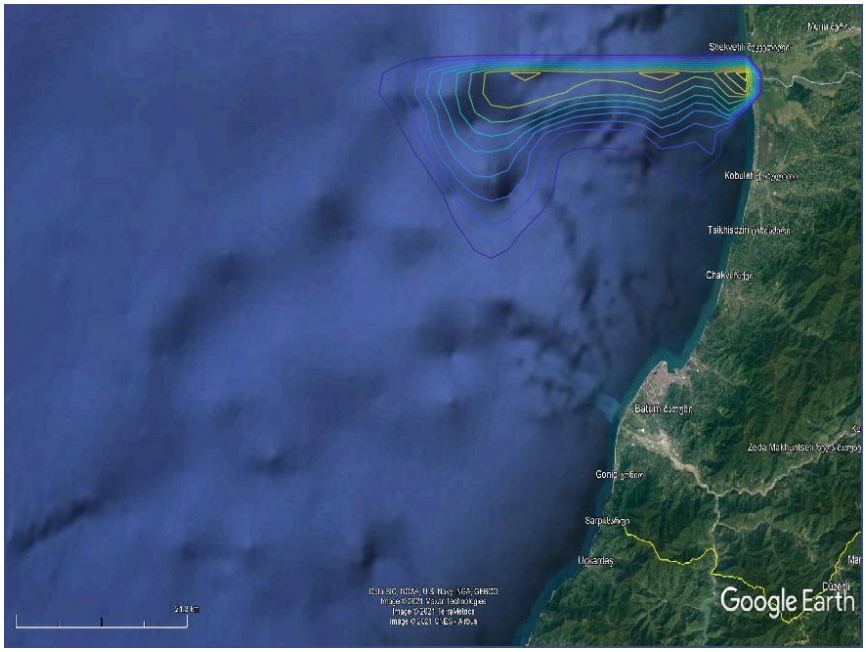

Figure 92: Result of Southwest wind condition for Choruhi River

Then, litters were reduced 10%, 30% and 70%. The results of these simulations are given in Figure 93.

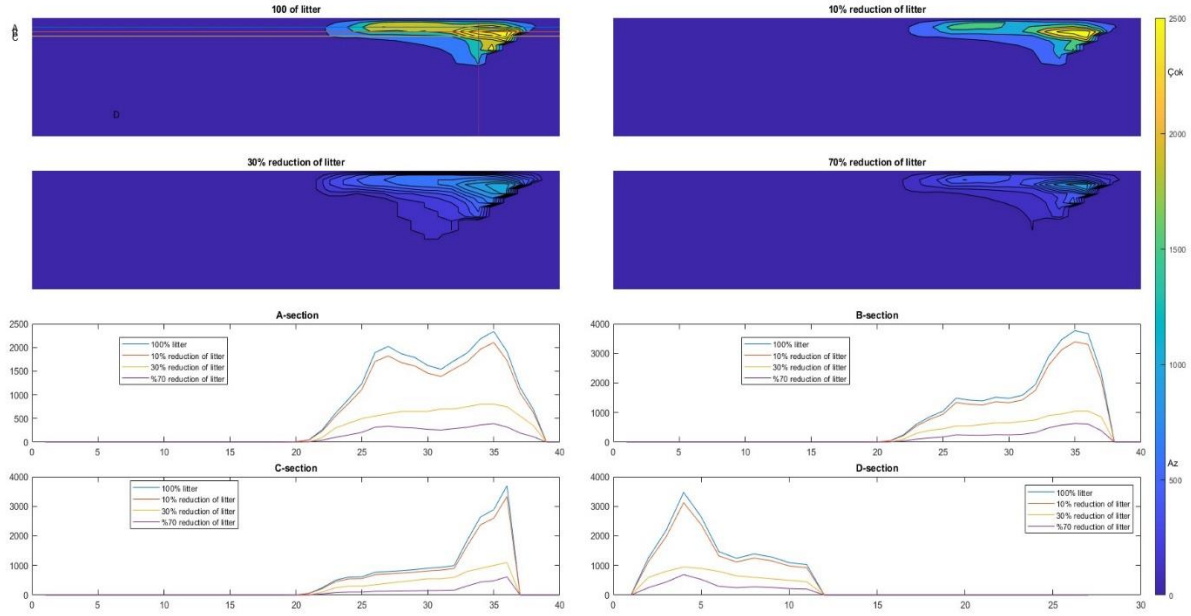

Figure 93: Litter distributions after %10, %30 and 70%reductions with SW wind direction

4.6.2.7 Wind Direction: West (W)

The following figure shows the simulation results of West wind conditions after a day (Figure 94).

Figure 94: Result of west wind condition for Choruhi River

Then, litters were reduced 10%, 30% and 70%. The results of these simulations are given inFigure 95.

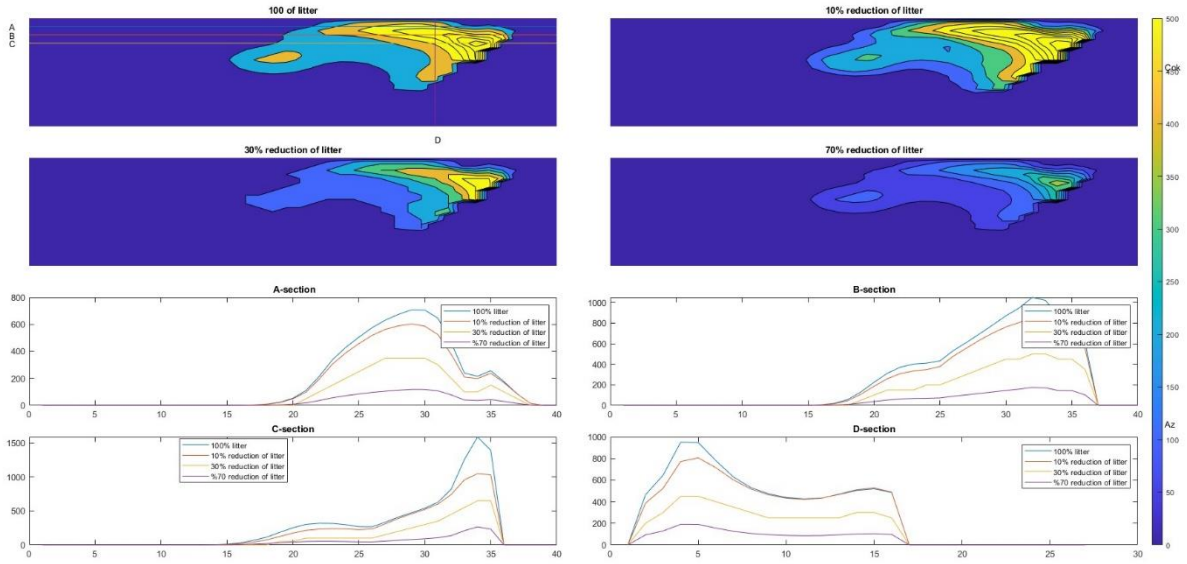

Figure 95: Litter distributions after %10, %30 and 70%reductions with SW wind direction

4.6.2.8 Wind Direction: North-West (NW)

The following figure shows the simulation results of North-West wind conditions after a day (Figure 96).

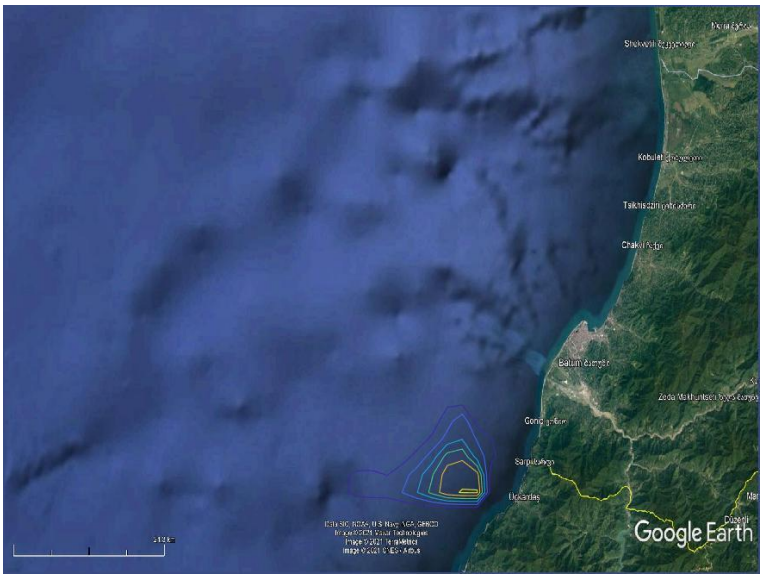

Figure 96: Result of Northwest wind condition for Choruhi River

Then, litters were reduced 10%, 30% and 70%. The results of these simulations are given inFigure 97.

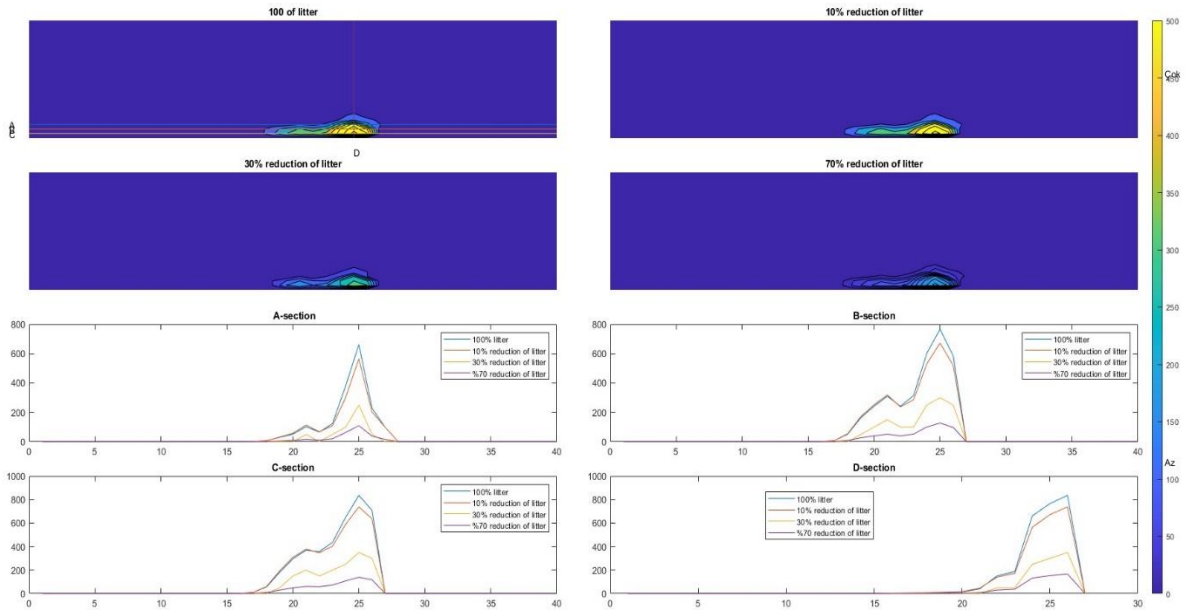

Figure 97: Litter distributions after %10, %30 and 70%reductions with NW wind direction

5 REFERENCES

[1] "Manahoz Deresi," enerjiatlası.com, 2019.

[2] "https://tr.wikipedia.org/wiki/%C3%87oruh," wikipedia.org.

[3] D. D. 2. B. M. -. ARTVİN, "Çoruh Nehri," 2015.

[4] "https://www.britannica.com/place/Danube-River," h/www.britannica.com.

[5] "http://www.ccpo.odu.edu/POMWEB/".

[6] "https://webapp.navionics.com/?lang=en#boating@6&key=sndyFoyrqF".

[7] "Statistical Yearbook 2017," National Statistical Institute (Bulgaria).

[8] "Report on "The Biological Diversity of the Black Sea Shelf Along the Bulgarian Coast and Its Adjacent Landscape," World Wildlife Fund, Retrieved 2008-11-21.

[9] "UN Economic Commission for Europe, Our waters: joining hands across borders : first assessment of transboundary, p, 150".